UNIVERZITA PALACKÉHO V OLOMOUCI
Přírodovědecká fakulta
Katedra optiky

VOJTĚCH KUPČÍK
V. ročník - prezenční studium

Obor: Optika a optoelektronika

GENERACE KVANTOVÉ PROVÁZANOSTI ASISTOVANÁ TERMÁLNÍM ŠUMEM

Diplomová práce

Vedoucí práce: Doc. Mgr. Radim Filip, Ph.D.

OLOMOUC 2015

PALACKÝ UNIVERSITY OLOMOUC
Faculty of Science
Department of Optics

VOJTĚCH KUPČÍK
5^{th} grade - Full-time study

Study Program: Optics and optoelectronics

QUANTUM ENTANGLEMENT GENERATION ASSISTED BY THERMAL NOISE

Master´s thesis

Supervisor: Doc. Mgr. Radim Filip, Ph.D.

OLOMOUC 2015

Tímto prohlašuji, že jsem tuto diplomovou práci vypracoval samostatně a použil jen uvedených zdrojů a literatury. Tímto také souhlasím se zveřejněním práce.

V Olomouci dne 10.4.2015 Vojtěch Kupčík

I hereby declare that this master´s thesis is completely my own work and that I used only the cited sources. I also agree with publishing of this thesis.

Olomouc, April 10, 2015 Vojtěch Kupčík

Tímto bych chtěl poděkovat Doc. Mgr. Radimu Filipovi, Ph.D., vedoucímu diplomové práce, za mnoho užitečných rad, trpělivost a podporu.

I would like to thank Doc. Mgr. Radim Filip, Ph.D., the supervisor of this master´s thesis for numerous useful advices, patience and support.

Contents

Chapter 1

ABSTRACT

There is an increasing effort in modern physics to connect different physical platforms. Such a quantum interconnection is based on the existence of entanglement between various systems. Quantum correlations between two physically different systems are an interesting phenomenon to study. They can provide an operational tools to manipulate limitedly accessible experimental platforms, such as noisy macroscopic atomic or mechanical systems, at quantum noise level using well controllable strongly quantum probes.

In this thesis, we propose and study a robust method of achieving basic QND interaction between continuous variables of two quantum oscillators A, B through the mediating oscillator M appearing in any unknown state. The mediating system is considered not to be accessible in other way than just by that QND interaction. This interaction allows to generate significantly entangled Gaussian states for any initial thermal noise of the mediating oscillator M. Moreover, we extensively analyze a robustness of the entangling procedure under small damping in the oscillators A,B and M in a limit of large noise of M. The proposed method can be used to construct optical microwave transducers, assisted by a noisy mechanical oscillator.

Chapter 2

THEORY

2.1 INTRODUCTION TO THE PROBLEM

In 1935, Austrian theoretical physicist Erwin Schrödinger proposed a thought experiment in order to demonstrate the problem he saw in the Copenhagen interpretation of quantum mechanics. It is named after him - the Schrödinger cat experiment.

To introduce the problem we closely follow the popular interpretation which can be found in [1]. Imagine a non-transparent box that is perfecly isolated from outer space. Once the box is closed, it is impossible to get any information about the inside without opening it. Inside of it we place a cat along with a device that contains radioactive source, a hammer and a flask which contains a poison. The experiment is constructed in the way that after a period of time there is a 50 percent chance of decaying the radioactive atom. If an internal counter detects radiation, the hammer breaks the flask with the poison and the cat is killed. Because of the perfect isolation of the box any observer has no imformation about what is happening inside, whether or not an atom has decayed, and consequently, whether the poison has been released, and the cat killed. According to the law of quantum physics and because we have not any knowledge about the inside, the cat is both dead and alive.

This configuration is called a *superposition* of states between the atom and the cat. Although the superposition of microscopic objects are commonly considered in quantum mechanics, here we speculate about the superposition of microscopic atom and macroscopic cat. The superposition is destroyed exactly at the momment when someone opens the box and the cat becomes one or the other (alive or dead). We influence the state of the system by opening the box, and therefore we make the wave function collapse. Schrödinger cat

experiment presents an interesting connection between a macroscopic system described by classical physics (the cat) and a system described by quantum laws (the radioactive atom). In fact, this thought experiment demonstrates a theoretical possibility of transposing non-classical features to strongly classical system. The main problem remaining in this though experiment is a definition of macroscopic (classical) system. In our considerations, we focus on initial macroscopic states represented by strongly mixed systems at thermal equilibrium with its environment. It is our step towards more serious discussion about the macroscopic quantum effects. Through the whole thesis, the term *entanglement* plays a key role in describing two-system states after an interaction. It is worth mentioning that Schrödinger coined this term (in German - Verschränkung) during the development of this experiment. We therefore consider the most feasible and robust type of Gaussian entanglement between two or more quantum oscillators, one quantum colled down to a ground state and another classical at thermal equilibrium with environment at room temperature.

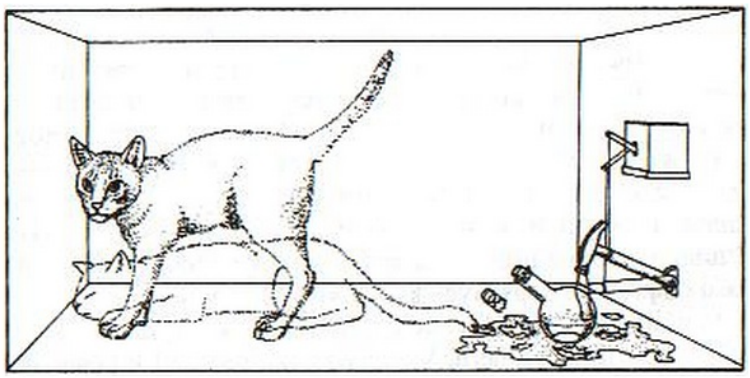

Figure 2.1: Schrödinger cat experiment. Since we can not gain any information about the inside of the box, the cat is in a superposition state with the radioactive atom, it is both dead and alive. [1]

In the same year as E. Schrödinger presented his thought experiment, another important paper was published. It is a significant and influential work written by A. Einstein, B. Podolsky and N. Rosen (EPR). Understanding of EPR paradox and the role of entanglement in it contributed to form a proper theoretical background of this thesis, therefore it is undoubtedly useful to mention it in the introduction. But since it was not our main motivation we introduce the concept very briefly, detailed description can be found in [2]. The main purpose of EPR paper was to show the incompleteness of quantum mechanics. The authors tried to show the possibility

of measuring position and momentum of a quantum particle at the same time, which is in contradiction to Heisenberg´s uncertainty principal. Although, the EPR paradox has been fully explained, it stimulated a birth of the method of remote state preparation based on the existence of entanglement. The remote state preparation is able to prepare a set of eigenstates of complementary variables (like position and momentum) on system A by an adjustable measurement on system B, if A and B are quantum-mechanically correlated.

Situation analogous to the Schrödinger cat experiment was the starting point and also the initial model for thermal entanglement analysis in [18]. In my bachelor´s thesis, we proposed a Gaussian version of the Schrödinger cat experiment. We demonstrated that these states are theoretically achievable even for highly noisy macroscopic system. Further analysis performed at our Department verified feasibility of thermal Gaussian entanglement in current quantum electromechanical systems. It demontrates a feasibility of Gaussian version of strongly mixed Schrodinger cat state. It is therefore possible to go beyond purely academic discussions and search for an interesting application of this entanglement.

The model situation for this master´s thesis is given by extended configuration of Schrödinger´s experiment. The current model contains a third additional quantum system coupled to the classical system. Imagine, for example, another atom A2 which can be coupled to already existing entangled state of the atom A1 and the cat. In principle, these two systems can be physically different if they can couple to the same classical mediating system M. It brings us to a concept of quantum transducer between different physical systems. The cat here stands as that mediator M of thermal entanglement. The goal is to gain quantum-mechanical correlations between two physical platforms represented by quantum systems (A1 and A2) without directly interacting with each other. Analogically to the Gaussian Schrödinger cat experiment where we build entanglement between quantum and classical system, initially at thermal equilibrium with the environment, here entanglement can be built with the third system using the classical one initially in thermal equilibrium.

2.2 INTERACTION OF LIGHT AND MECHANICAL OSCILLATOR

Let´s consider a typical scheme for quantum optomechanics - a cavity with a movable mirror at one end. Everytime a photon reflects on the movable

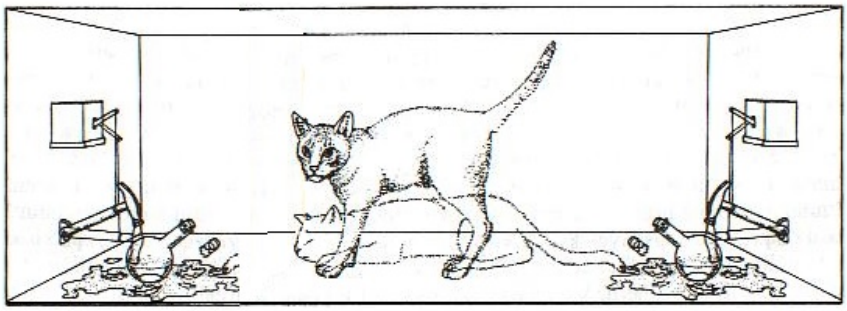

Figure 2.2: The idea of extended configuration of Schrödinger cat experiment. Third system is included and the cat participates in the interaction only as a mediator. The goal is to build entanglement between two quantum systems without directly interacting with each other.

mirror, it transfers energy onto the mirror and thus makes the mirror vibrate (slightly changes the position of the mirror). We say that the light transfers energy through a radiation pressure.

The radiation pressure interaction can now be used to modify the dynamics of the mechanical oscillator. We can model this situation as a coupling between a mechanical and an optical oscillator. In microscopic terms we can imagine that optical oscillator - mode of light and mechanical oscillator - mode of vibrations, exchange photon to phonon and vise versa. We consider here the case that we are able to detect a single cavity mode and also a single mechanical mode only and that the mechanical modes do not couple to each other. In this section we closely follow the derivation presented in [3].

2.2.1 OPTICAL RESONATOR

To characterize an optical cavity we introduce a few relevant parameters. The cavity contains a series of resonances $\omega_{cav} = m\pi(c/L)$, where L is the distance between the mirrors and m being an integer number. The free spectral range (FSR) of the cavity is defined as the separation of two longitudinal resonances

$$\Delta\omega_{FSR} = \pi\frac{c}{L}. \tag{2.1}$$

A photon cavity decay rate κ describes the energy losses caused by finite mirror transparencies and the absorption inside the cavity. An average number of cycles that photon makes inside the cavity before leaving it, is desribed by the quantity

$$F \equiv \frac{\Delta\omega_{FSR}}{\kappa}, \tag{2.2}$$

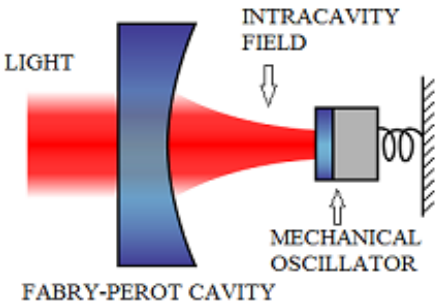

Figure 2.3: Radiation pressure interaction. Light is coupled through an input mirror into a resonator with a movable mirror in the back, it transfers energy onto the mirror via radiation pressure [4].

which is called optical finess. As an alternative, we can introduce a quality factor of the optical resonator

$$Q_{OPT} = \omega_{cav}\tau, \tag{2.3}$$

where $\tau = \kappa^{-1}$ is the photon lifetime. If we consider a high-Q cavity, its decay rate can be expressed as a sum of two separate components $\kappa = \kappa_{ex} + \kappa_0$, where κ_{ex} refers to the loss rate associated with the input coupling and κ_0 represents the remaining loss rate.

A quantum mechanical description of a cavity coupled to the environment can be given by a framework known as input-output formalism of quantum theory [3]. It describes the time evolution of the field amplitude $\hat{c}$ inside the cavity. The formalism is formulated on the level of a modification of Heisenberg-Langevine equations of motion. The equation of motion in input-output formalism reads

$$\dot{\hat{c}} = -\frac{\kappa}{2}\hat{c} + i\Delta\hat{c} + \sqrt{\kappa_{ex}}\hat{c}_{in} + \sqrt{\kappa_0}\hat{f}_{in}, \tag{2.4}$$

where $\hat{c}_{in}$ is the annihilation operator of single input cavity mode and $\hat{f}_{in}$ is Langevin operator of external environment of cavity. The classical analogy to this equation could be obtained by simply taking the average value of the operators. We use a frame rotating with the laser frequency ω_L, which means $\hat{c} = e^{-i\omega_L t}\hat{a}$ and introduce the laser detuning $\Delta = \omega_L - \omega_{cav}$. For a very good cavity, we can neglect κ_0 and then all the intracavity field can be asymptotically obtain in the output mode. According to the input-output

theory of open quantum systems , the field that is reflected from the Fabry-Perot resonator is given by

$$\hat{c}_{out} = \hat{c}_{in} - \sqrt{\kappa_{ex}}\hat{c}. \tag{2.5}$$

One can find numerous textbooks with detailed discussion of quantum treatment of optical fields, e. g. [5],[6].

2.2.2 MECHANICAL RESONATOR

Now we focus on a single normal mechanical mode of vibration of frequency Ω_m. Analogically to the optical resonator we introduce relevant parameters that represent the energy damping in the oscillator. The mechanical oscillator is described by the damping rate Γ_m or the quality factor $Q_m = \frac{\Omega_m}{\Gamma_m}$. If we are interested in equation of motion for the global amplitude $x(t)$ of the osciallator, we can utilize a suitably normalized dimensionless mode function $\vec{u}(\vec{r}, t)$, such that the displacement field would be $\vec{u}(\vec{r}, t) = x(t) \cdot \vec{u}(\vec{r})$. The evolution is then described by a simple equation of motion for a harmonic oscillator of mass m:

$$m\frac{dx^2(t)}{dt^2} + m\Gamma_m\frac{dx(t)}{dt} + m\Omega_m^2 x(t) = F_{ex}(t). \tag{2.6}$$

The right side of this equation represents the sum of all the forces acting on the mechanical resonator.

The quantum mechanical treatment of the mechanical harmonic oscillator [7] leads to the Hamiltonian

$$\hat{H} = \hbar\Omega_m(\hat{b}^+\hat{b} + \frac{1}{2}), \tag{2.7}$$

where $\hat{b}^+(\hat{b})$ are the phonon creation (anihilation) operators. We define

$$\hat{x} = x_{ZPF}(\hat{b}^+ + \hat{b}),$$
$$\hat{p} = -im\Gamma_m x_{ZPF}(\hat{b} - \hat{b}^+),$$

where

$$x_{ZPF} = \sqrt{\frac{\hbar}{2m\Gamma_m}}$$

is the zero point fluctuation amplitude of the mechanical oscillator. The position and momentum satisfy $[\hat{x}; \hat{p}] = i\hbar$. We typically do not display the contribution of the zero-point energy to the energy of the oscillator.

2.2.3 OPTOMECHANICAL COUPLING

In our case the coupling between mechanical and optical oscillator is performed by the radiation pressure. A single photon transfers the momentum $|\Delta p| = 2\hbar/\lambda$, λ being the light wavelength. The radiation pressure force is therefore given by [3]

$$\langle \hat{F} \rangle = 2\hbar k \frac{\langle \hat{a}^+ \hat{a} \rangle}{\tau_c} = \hbar \frac{\omega_{cav}}{L} \langle \hat{a}^+ \hat{a} \rangle. \tag{2.8}$$

Here $\tau_c = 2L/c$ denotes the cavity round-trip time.

The Hamiltonian of two uncoupled modes is given simply as the sum of individual Hamiltonians

$$\hat{H}_0 = \hbar\omega_{cav}(x)\hat{a}^+\hat{a} + \hbar\Omega_m \hat{b}^+\hat{b}. \tag{2.9}$$

The radiation pressure makes the movable mirror change its position, the length of the cavity increases and the resonance frequency of the cavity changes. The coupling is therefore parametric

$$\omega_{cav}(x) \approx \omega_{cav} + x\frac{\partial \omega_{cav}}{\partial x} + \cdots.$$

For our discussion it is sufficient to keep the linear term, where we define the optical frequency shift per displacement as $G = -\frac{\partial \omega_{cav}}{\partial x}$. Expanding to the leading order in the displacement we obtain

$$\hbar\omega_{cav}(x)\hat{a}^+\hat{a} \approx \hbar(\omega_{cav} - G\hat{x})\hat{a}^+\hat{a}. \tag{2.10}$$

Using earlier definition of $\hat{x} = x_{ZPF}(\hat{b}^+ + \hat{b})$ we get the form of interaction Hamiltonian

$$\hat{H}_{int} = -\hbar g_0 \hat{a}^+\hat{a}(\hat{b}^+ + \hat{b}), \tag{2.11}$$

where $g_0 = G x_{ZPF}$ is the vacuum optomechanical coupling strength. Since the coupling strength is exremely low, we can enhance it using a combination of the cavity effect and large intensity of the coherent pump. The necessary consquence of this increase of coupling strength is the linearization of (2.11). We rewrite the amplitude of the optical field as a sum of an average coherent amplitude $\bar{a}$ and a fluctuating term $\delta\hat{a}$:

$$\hat{a} = \bar{a} + \delta\hat{a}. \tag{2.12}$$

Inserting this new form of the optical field in (2.11) we get

$$\hat{H}_{int} \propto (\bar{a} + \delta\hat{a})^+(\bar{a} + \delta\hat{a})(\hat{b}^+ + \hat{b}). \tag{2.13}$$

This expression can be expanded in terms of $\bar{a}$. The first term $\propto |\bar{a}|^2$ can be omitted after implementing an appropriate shift of the mechanical displacement´s origin and afterward always using a modified detuning. The second term, of order $|\bar{a}|$, is the one we focus on and the third term is ignored because of being smaller by factor $|\bar{a}|$. Assuming that $|\bar{a}|$ is a real number, the resulting interaction Hamiltonian reads

$$\hat{H}_{int} \propto (\delta\hat{a}^+ + \delta\hat{a})(\hat{b}^+ + \hat{b}). \tag{2.14}$$

It is a qudratic Hamiltonian of QND type which rises from linearization of original nonlinear cubic Hamiltonian for the pressure of light. It is advantageous for us because it leads to linear Heisenberg-Langevine equations of motion for the optomechanical interaction. Such linear equations have a linear solutions in the operators of the systems which transform Gaussian states always to Gaussian states.

2.3 PULSED OPTOMECHANICS

There have been numerous various experiments proposed and performed in quantum optomechanics [8],[9],[10]. To present a scheme close to our proof-of-principle considerations in following sections the pulsed regime of quantum optomechanics is used.

Through this work we frequently mention [11] as a stimulating idea. In the last chapter of this thesis we propose an experiment that is a modification of the one in [11]. It is therefore convenient to use this experiment for demonstration of basic properties of pulsed optomechanics. In following chapter we also include a brief overview of the whole experiment in order to show the analogy to this work.

A specific feature of pulsed optomechanics is an optical pump which consists of very intensive short pulses. There are important limitations in the experiment parameters that have to be satisfied to fully utilize possibilities that pulsed regime provides. In [11], the experiment consists of four consequent interactions between laser pulse and mechanical oscillator. The required constraints read

$$T_M \gg \tau > 4\sigma > \kappa^{-1}, \tag{2.15}$$

where $T_M = 2\pi/\Omega_m$ is the period of motion of the mechanical oscillator, τ stands for the round-trip time of each laser pulse, σ is the temporal width

of laser pulse and κ represents the photon cavity decay rate. Expr. (2.15) contains three simultaneous inequalities, each of them represents a different experimental limitation. For each interaction it is assumed, that the pulse has the same teporal profile, which is valid if $\sigma > \kappa^{-1}$. Setting $\tau > 4\sigma$, ensures that each successive pulse decays out of the cavity prior to the next pulse entering. This also enables to neglect interference between subsequent pulses and successfully resolve individual interactions. Finally, to generate geometric phase effect exploited in our method we need the mechanical oscillator to be nearly motionless, which is represented by $T_M \gg \tau$. The laser pulse also has to be shorter than decoherence time of the present field and the mechanical oscillator. In this regime, we can simply neglect the free evolution of mechanics and all mechanical noise effects. The free evolution of optical mode can be eliminated by setting the verification of light mode at the same frequency. The coupling is then a simple QND coupling between light and mechanics.

Optomechanical coupling does not necessarily require a cavity, however its presence appears to enhance the coupling strength [9]. The experiment reported in [9] is performed in the regime satisfying (2.15). The experiment uses Mach-Zehnder interferometer that has a micro-mechanical oscillating mirror in one of the two interferometer paths. The pulses are first divided by a beam-splitter into a weak signal beam and an intense beam. The intense beam acts as a local oscillator, wheres the signal beam is focussed onto the mirror. The coherent optical pulse gains a phase shift proportional to the mechanical position. Concurrently, the radiation pressure imparts momentum onto the mirror. The imformation exchange between the light and mechanics is quantified by $\chi = 4\pi x_0\sqrt{N}/\lambda$. [$N$, mean photon number per pulse; λ, optical wavelength; $x_0 = (\hbar/2m\Omega_m)^{1/2}$, mechanical ground state extension; m, mechanical mass; Ω_m, mechanical angular frequency]. The authors specified all the elements used in experiments, we do not include these parameters here. For tha largest optical pulse strength used the measured results correspond to the interaction strength of $\chi \propto 10^{-4}$. An effective way to increase this quantity is to employ an optical cavity to enhance the optomechanical interaction. Using the same experimental parameters, a cavity of finesse $\propto 10^4$ is sufficient. As such a cavity simultaneously requires a high finesse, as well as a large bandwith to accomodate a short optical pulse, this is best achieved with an optomechanical microcavity [3].

2.4 COHERENT, SQUEEZED AND THERMAL STATES

In this thesis we deal only with Gaussian states, they are enough to describe quantum oscillators cooled down to ground state as well as the thermal states of oscillators at thermal equilibrium. In order to understand the difference between classical and non-classical states it is convenient to present their definitions [5]. To be able to define that difference it is necessary to know the term *coherent state*. Coherent states build a connection between quantum and classical coherence theory in the sense that they are the most appropriate quantum representation of a classical wave. Differently to the thermal equilibrium states, the coherent states are out of the thermal equilibrium.

Let´s start with the classical oscillator, it can be described by the correlation function for all possible times

$$\langle \alpha^{*n}(t)\alpha^{m}(t')\rangle, \tag{2.16}$$

with an amplitude α. Moving to the quantum oscillator we deal with the creation $\hat{a}^{+}$ and the annihilation $\hat{a}$ operators(for simplicity we no longer use the notation $\hat{a}$ and reduce it to simple a)

$$\langle a^{+n}(t)a^{m}(t')\rangle. \tag{2.17}$$

These two expressions should correspond

$$\langle \alpha^{*n}(t)\alpha^{m}(t')\rangle = \langle \psi|a^{+n}(t)a^{m}(t')|\psi\rangle, \tag{2.18}$$

therefore coherent state $|\alpha\rangle$ is an eigenstate of the annihilation operator $a|\alpha\rangle = \alpha|\alpha\rangle$.

The definition says that classical state is a mixture of coherent states

$$\rho = \int P(\alpha)|\alpha\rangle\langle\alpha|d^2\alpha, \tag{2.19}$$

whereas non-classical states $\rho \neq \int P(\alpha)|\alpha\rangle\langle\alpha|d^2\alpha$ are not compatible with such an expansion.

Thermal states are an example of classical states being at thermal equilibrium with the environment. These states can be desribed as states with maximal entropy and constant average value of energy. It is defined in Fock state representation by the density operator

$$\rho = \sum_{n} \frac{\langle n\rangle^{n}}{(1+\langle n\rangle)^{n+1}}|n\rangle\langle n|, \tag{2.20}$$

where

$$\langle n\rangle = \frac{1}{e^{\frac{\hbar\Omega_m}{kT}} - 1} \tag{2.21}$$

is the average value of number operator, $\hbar$ is a reduced Planck constant, Ω_m is the oscillator frequency, k is a Boltzmann constant and T stands for the ambient temperature. In the representation of coherent state the definition reads

$$\langle\alpha|\hat{\rho}|\alpha\rangle = \sum_n \frac{\langle n\rangle^n}{(1+\langle n\rangle)^{n+1}}\langle\alpha|n\rangle\langle n|\alpha\rangle = \frac{e^{-|\alpha|^2}}{1+\langle n\rangle} e^{\frac{-|\alpha|^2}{1+\frac{1}{\langle n\rangle}}}. \tag{2.22}$$

Thermal states are also characterized by zero average value of its quadratures $\langle x\rangle = \langle p\rangle = 0$ and equal variances $V_x = V_p = \langle x^2\rangle = \langle p^2\rangle$. Variance of the number operator reads

$$V_N = \langle n\rangle(1+\langle n\rangle). \tag{2.23}$$

It is illustrative to include a dependance of the thermal noise V_N on the ambient temperature and the frequency of the mechanical ocsillator, which is illustrated in Fig. 2.4. Phonon statistics is described by Bose-Einstein distribution (2.21). If we use the form of the creation $a^+ = \frac{x-ip}{2}$ and the annihiliation $a = \frac{x+ip}{2}$ operator and consider the commutator $[x,p] = 2i$ and the fact that $\langle x^2\rangle = \langle p^2\rangle = V_N$, we obtain the expression that enables to determine the value of V_N

$$V_N = \frac{2}{e^{\frac{\hbar\Omega_m}{kT}} - 1} + 1. \tag{2.24}$$

We include this figure for better imagination of scale we use in graphs that illustrate our results. It is clear that for lower frequencies of mechanical oscillator the variance V_N can be much larger than unity, even quite below a room temperature. It very simply demonstrates the importance of robustness of procedures under the thermal mechanical noise.

Coherent states, i. e. states of the field that correspond to the classical oscillations the best, started to attract attention with the invention of laser and also with the huge development of quantum theory. In classical theory the oscillations have well-defined amplitude and phase. The transition from classical to quantum physics brings fluctuations associated with both amplitude and phase. We can describe the field in terms of the two conjugate quadrature components. They are limitted by fundamental Heisenberg´s uncertainty principle which is in the form:

$$V_x V_p \geq 1, \tag{2.25}$$

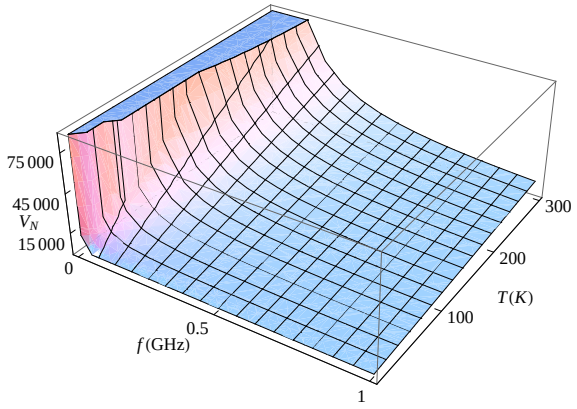

Figure 2.4: The dependance of the thermal noise V_N on the ambient temperature T and the frequency $f = \Omega_m/2\pi$.

where V_x and V_p stand for the variance in position $x = a + a^+$ or in momentum $p = i(a - a^+)$, respectively. Both variables x and p for both optical and mechanical oscillator are identically decomposing the annihilation operator $a = \frac{x+ip}{2}$ of photons and phonons. A field in a *coherent state* satisfies the minimum-uncertainty equation and also has equal uncertainties in both quadrature components.

In principle, there is a possibility of generating a state that satisfies the lowest limit for uncertainty but does not have symmetrical fluctuations. It means that the field in this state has a single variance of the quadrature components reduced below unity. This fact is compensated by increasing variance in the conjugate quadrature, such that the Heisenberg´s uncertainty relation is not violated. Such states of a radiation field are called *squeezed states*, which can be obtained by unitary trasformation of the coordinate and momentum variables $x' = \lambda x$, $p' = \lambda^{-1} p$, where $\lambda \in (0, \infty)$. Two cases can occur, if $\lambda < 1$ the state is squeezed in x, or $\lambda > 1$ and the is state squeezed in p. A quadrature component with fluctuations that are below the standard quantum limit, has interesting aplications in gravitational wave detection [12], quantum teleportation [13] and quantum computing [14].

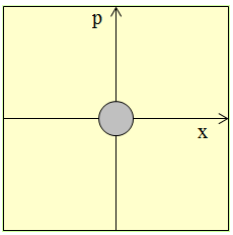

Figure 2.5: vacuum [15]

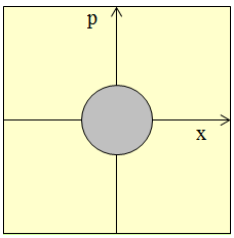

Figure 2.6: a thermal state [15]

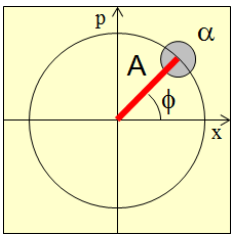

Figure 2.7: a coherent state [15]

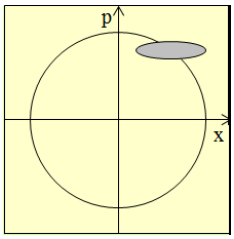

Figure 2.8: a squeezed state [15]

2.5 QUADRATURE PICTURE OF QND INTERACTION

Single modes of mechanical and optical resonators can be considered as a quantum harmonic oscillator. If we assume a regime of a strong optical pumping, when there is enough strong and fast coupling between light and matter to be almost unitary, it still keeps much lower strength than a perfect swap of quantum states between light and matter would require. Using frequency detuning of mechanical oscillator and optical mode, this coupling can be modificated among very different types of quadratic interactions [3]. It includes all the three prominent interactions: beam-splitter (BS), amplifier (AMP) and quantum non-demolition (QND), which will be our main focus.

We describe the interaction between two physical systems A and B as the simplest but weak Gaussian interaction between two different linear harmonic quantum oscillators described by X_A, P_A and X_B and P_B, respectively. They satisfy $[X, P] = 2i$.

The asymmetrical unitary QND interaction can be adjusted by local phase shift to the two different transformations, either

$$X'_A = X_A \ , P'_A = P_A - KP_B,$$

$$X'_B = X_B + KX_A \ , P'_B = P_B \tag{2.26}$$

transfering X_A to the mechanical oscillator B, or

$$\begin{aligned} X'_A &= X_A + KP_B \ , P'_A = P_A, \\ X'_B &= X_B + KP_A \ , P'_B = P_B \end{aligned} \tag{2.27}$$

transferring P_A to the mechanical oscillator B, with QND gain $K > 0$. A weak interaction is represented by the value of K close to the zero. Here we consider for simplicity that optomechanical interaction is enhanced enough to make free evolution negligible during the coupling.

2.6 THE COVARIANCE MATRIX, ENTANGLEMENT AND CONDITIONAL VARIANCE

To introduce these terms we follow [16].

2.6.1 GAUSSIAN ENTANGLED STATES, THE COVARIANCE MATRIX

To describe Gaussian entanglement generated between two modes assisted by mediator, we will introduce the formalism of covariance matrices useful to calculate logarithmic negativity as a reasonable measure of the Gaussian entanglement. For describing a continuous variable (CV) system we use a Hilbert space resulting from the tensor product of infinite dimensional Fock spaces. Using the annihilation and the creation operators is convenient here. Let these operators act on each Fock space and define the related quadrature phase operators $\hat{x}_j = (a_j + a_j^+)$, $\hat{p}_j = i(a_j - a_j^+)$. We denote x_j and p_j the corresponding phase space variables. Let $\hat{X} = \hat{x}_1, \hat{p}_1, ..., \hat{x}_n, \hat{p}_n$ denote the vector of the operators $\hat{x}_j$ and $\hat{p}_j$. In terms of the symplectic form Ω, the commutation relations for the $\hat{X}_j$ take the form

$$[\hat{X}_j, \hat{X}_k] = 2i\Omega_{jk},$$

with

$$\Omega \equiv \bigoplus_{j=1}^{n} \omega, \omega \equiv \begin{pmatrix} 0 & 1 \\ -1 & 0 \end{pmatrix}.$$

Such a CV system could be also described by a positive trace-class operator (the density matrix ρ). In this thesis, we deal only wit Gaussian states and Gaussian interactions. Gaussian states are fully described by their first and second statistical moments of the field operators, because higher moments are determined by them. Each physical system in our discussion is therefore characterized by the variance of x and p. If the Gaussian character of both systems is preserved after the interaction, we describe it as a Gaussian interaction.

To investigate entanglement generation between two systems it is necessary to introduce the covariance matrix (CM) formalism. The covariance matrix Γ consists of elements that are defined as

$$\Gamma_{jk} \equiv \frac{1}{2}\langle \hat{X}_j \hat{X}_k + \hat{X}_k \hat{X}_j \rangle - \langle \hat{X}_j \rangle \langle \hat{X}_k \rangle. \tag{2.28}$$

Apparently, covariance matrix resulting from this definition is symmetrical. According to the earlier definition of the quadrature operators in terms of the ladder operators, the entries of CM are real numbers. The canonical commutation relations and the positivity of the density matrix ρ imply

$$\Gamma + i\Omega \geq 0, \tag{2.29}$$

meaning that all the eigenvalues of the matrix $(\Gamma + i\Omega)$ have to be greater or equal than zero. This expression is very powerful because it is a necessary and sufficient condition the matrix Γ has to fulfil to be the CM corresponding to a physical state. Notice that Ineq.(2.29) is the constraint for any states (not only for the Gaussian states). For pure, uncorrelated states it reduces to a familiar Heisenberg´s principle. Such a restriction implies $\Gamma \geq 0$.

2.6.2 TWO-MODE STATES

In our discussion we concetrate on two-mode Gaussian states. Basic properties of such states are listed below. Any covariance matrix can be devided in sub-matrices. In case of two-mode state it is useful to express the CM in terms of three 2×2 matrices α, β and γ

$$\Gamma \equiv \begin{pmatrix} \alpha & \gamma \\ \gamma^T & \beta \end{pmatrix}. \tag{2.30}$$

Matrices α and β contain information about each system, whereas γ consists of correlations between them. In principle, for any two-mode CM Γ we can find local symplectic operations S_1 and S_2 (each S_j acting on one of the two modes) that their direct sum $S_1 \bigoplus S_2$(corresponding to the tensor product of local unitary operations) changes the CM Γ to the so called standard form Γ_{sf}

$$S_l^T \Gamma S_l = \begin{pmatrix} a & 0 & c_+ & 0 \\ 0 & a & 0 & c_- \\ c_+ & 0 & b & 0 \\ 0 & c_- & 0 & b \end{pmatrix}. \tag{2.31}$$

The states with $a = b$ are called symmetric. Further, any pure state is symmetric and fulfils $c_+ = -c_- = \sqrt{a^2 - 1}$. Notice, that up to a common sign flip between c_+ and c_-, the standard form associated with any CM is unique. It is unique because the correlations a, b, c_+, c_- are determined by the four local symplectic invariants $Det\Gamma = (ab - c_+^2)(ab - c_-^2), Det\alpha = a^2, Det\beta = b^2, Det\gamma = c_+ c_-$. Considering two-mode states, the Ineq.(2.29) can be recast as a constraint $Sp_{(4,R)}$ invariants $Det\Gamma$ and $\Delta(\Gamma) = Det\alpha + Det\beta + 2Det\gamma$:

$$\Delta(\Gamma) \leq 1 + Det\Gamma. \tag{2.32}$$

We denote ν_- and ν_+ the symplectic eigenvalues of the CM corresponding to a two-mode Gaussian state. With the convention $\nu_- < \nu_+$, the Heisenberg uncertainty relation reducing to

$$\nu_- \geq 1. \tag{2.33}$$

The expression for determining the symplectic eigenvalues is

$$\nu_\mp = \sqrt{\frac{\Delta(\Gamma) \mp \sqrt{\Delta(\Gamma)^2 - 4Det\Gamma}}{2}}. \tag{2.34}$$

The physical meaning of the smallest symplectic eigenvalue appears in a connection with entanglement presented in the state.

2.6.3 ENTANGLEMENT OF GAUSSIAN STATES

To be able to separate two-mode Gaussian states it is necessary and sufficient to satisfy the positivity of the partially transposed states (PPT criterion). The partial transposition of a bipartite quantum state is defined as a simple

transposition but applied only on one of the two subsystems in a given basis. In our case this leads to a sign flip in $Det\gamma$. Therefore $\Delta(\Gamma)$ changes to $\tilde{\Delta}(\Gamma)$, that takes the form

$$\tilde{\Delta}(\Gamma) = Det\alpha + Det\beta - 2Det\gamma. \tag{2.35}$$

The symplectic eigenvalue now reads

$$\tilde{\nu_{\mp}} = \sqrt{\frac{\tilde{\Delta}(\Gamma) \mp \sqrt{\tilde{\Delta}(\Gamma)^2 - 4Det\Gamma}}{2}}. \tag{2.36}$$

The PPT criterion thus reduces to a simple inequality that must be satisfied by the smallest symplectic eigenvalue $\tilde{\nu}_-$ of the partially transposed state

$$\tilde{\nu}_- \geq 1, \tag{2.37}$$

which can be equivalently written in the form

$$\tilde{\Delta}(\Gamma) \leq Det\Gamma + 1. \tag{2.38}$$

Looking at the above inequalities in detail, they imply $Det\gamma = c_+c_- < 0$ as the necessary constraint for generating entanglement for the two-mode Gaussian state. The quantity $\tilde{\nu}_-$ provides all the information about qualitative characterization of the entanglement for arbitrary two-mode Gaussian states. If the PPT criterion is violated, we automatically know that the systems are entangled which means that we are interested in the states that do not satisfy (2.37).

We presented a method that enables to decide if two systems are entangled. The next logical step is to determine how much entanglement is generated. In other words, how to characterize entanglement from the quantitative point of view. There are many different ways how to quantify entanglement, we would like to briefly introduce only few of them that suit our case best. A measurement of Gaussian entanglement can be provided by the negativity N. The negativity N of a state ϱ is defined as

$$\mathsf{N}(\varrho) = \frac{\|\tilde{\varrho}\| - 1}{2}, \tag{2.39}$$

where $\tilde{\varrho}$ is the partially transposed density matrix and $\|\hat{o}\| = Tr|\hat{o}|$ represents the trace norm of the hermitian operator $\hat{o}$. In our discussion, we use

logarithmic negativity E_N as the main indicator of how much entanglement is generated. It is strictly related to the negativity N and is defined as

$$\mathsf{E}_N \equiv log_2\|\tilde{\varrho}\|. \tag{2.40}$$

For any two-mode Gaussian states the negativity is a simple decreasing function of $\tilde{\nu}_-$, therefore it is an inverse quantifier of entanglement:

$$\|\tilde{\varrho}\| = \frac{1}{\tilde{\nu}_-} \Rightarrow \mathsf{N}(\varrho) = max[0, \frac{1-\tilde{\nu}_-}{2\tilde{\nu}_-}], \mathsf{E}_N = max[0, -log_2\tilde{\nu}_-]. \tag{2.41}$$

These expressions determine how strongly the PPT inequality (2.37) is violated. From these we can say that the symplectic eigenvalue $\tilde{\nu}_-$ completely qualifies and also quantifies the quantum entanglement of a Gaussian state. We would also like to mention another quantity called fidelity. It is not used in this work but we include it here for completeness. The fidelity sets how much successful a teleportation experiment is [13], it reaches unity only for a perfect transfer of a state. According to experiments, without using entanglement, by purely classical communication the fidelity of $\mathsf{F}_{CL} = \frac{1}{2}$ is the best that can be achieved. The sufficient fidelity criterion says that if teleportation is made with $\mathsf{F} > \mathsf{F}_{CL}$, then the shared resource is entangled. But converse statement is generally false. The optimal fidelity is given by

$$\mathsf{F}^{OPT} = \frac{1}{1+\nu_-}, \tag{2.42}$$

where ν_- is the smallest symplectic eigenvalue of CM. This equation shows that optimal fidelity of continuous variables teleportation of coherent states depends only on the entanglement quantified by ν_-. More information about fidelity can be found in [17].

2.6.4 CONDITIONAL VARIANCE

By conditional variance we understand a controllable preparation of a state in system A by measuring system B only. Furthermore, a preparation of a non-classical state in a classical system. Since our discussion is about Gaussian states the only way how to prepare a non-classical state is to squeeze the variance under unity. Therefore it is also referred as conditional squeezing. Mathematical expression takes the form

$$V_C = \langle (X_A - gX_B)^2 \rangle, \tag{2.43}$$

where g is a variable gain, which is used to reduce the variance $V_{XA} = \langle X_A^2 \rangle$ to V_C. It applies transformation of X_A to $X_A - g\bar{X}_B$, where $\bar{X}_B$ is a measured value of X_B.

In principle, we distinguish two types of conditional variance, but the difference is only how to achieve the required state. If we consider that $\langle X_B \rangle = \langle X_A \rangle = 0$ and minimalizing via g we obtain

$$V_C = \langle X_A^2 \rangle - \frac{|\langle X_A X_B \rangle|^2}{\langle X_B^2 \rangle}, \tag{2.44}$$

which means that in this type the key task is to optimize the factor g. On the other hand, the principle in the second case is in selecting appropriate measurement results. Whenever $X_B \approx 0$ is measured we know that we obtain the minimum conditional variance that is in agreement with (2.44). Any other results that are not in a very small interval around zero are just thrown away. Because of the selection of only a few measurements from a huge number of attempts this method is sometimes referred as probabilistic.

Chapter 3

THERMAL ENTANGLEMENT PRODUCED BY QND

The existence of entanglement between a quantum system and a macroscopic object is the defining feature of the interpretation of the Schrödinger cat state. We model the Schrodinger cat state by very robust Gaussian entanglement with a very noisy system at thermal equilibrium. The possibility of generating this thermal Gaussian entanglement and its consequent properties is discussed in [18] for three prominent types of interactions. The main purpose was to pick the most appropriate intearaction type that would show the most promising results. Our ambition here is to give a summary of the most significant results to identify the starting point of this master´s thesis.

Amplifier and QND generate entanglement for all possible values of the variances of variables in discussion, even for high values of thermal noise V_N. Beam splitter is the type of interaction that requires squeezed state at the input to observe entanglement at all, therefore it is clearly not a proper candidate to our purpose here. Of course, the amount of entanglemenent for $V_N \gg 1$ is very low for both amplifier and QND. However, it is never vanishing, therefore the interaction does not degrade to entanglement breaking. The only way to obtain more entangled state is to input squeezed state, where the amplifer shows slightly more promising result than QND. On the other hand, squeezing at the input of the light system decreases the robustness of entanglement against subsequent damping before further application for both QND and amplifier. Only amplifier presents the possibility of preserving entanglement through small energy losses even for $V_N \gg 1$. Also the conditional variance analysis showed the best state preparation of squeezed state of matter for the amplifier. In all three cases of various interactions, the noisy matter system shows higher robustness to energy damping.

Despite the fact, that amplifier was the best candidate to obtain robust

thermal entanglement, our analysis showed that it is inapplicable for the purposes of this thesis. On the other hand, the second best candidate - QND - enables configuration that is suitable for this situation and will be used through the whole thesis. It is therefore useful to review the properties of QND interaction more extensively.

3.1 GAUSSIAN ENTANGLEMENT FROM QND INTERACTION

The light is characterized by the variance $V_S \in (0; 1\rangle$ which determines its squeezing. To describe the thermal noise of the mechanical oscillator we use the variance $V_N > 1$. QND interaction advantageously generates entanglement for all configurations, which means the light does not have to be in a squeezed state and the mechanical system can contain a lot of noise to still observe entanglement after the interaction. The amount of entanglement for high values of V_N is however very low and the only way how to increase entanglement is to use squeezed state of light. This is illustrated in Fig. 3.1.

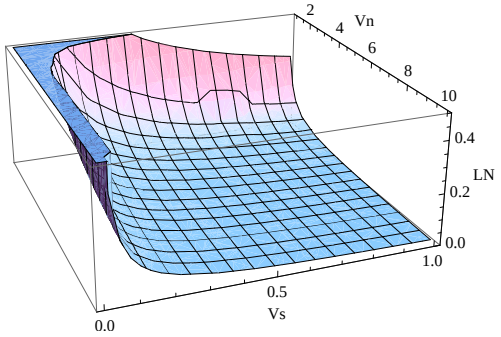

Figure 3.1: QND type of interaction ($K^2 = 0.05$): logarithmic negativity as a function of V_S and V_N.

The most illustrative and simple way how to characterize the realistic change of entanglement is to determine how quickly it increases when the squeezing goes from the threshold $V_S = 1$. QND is a non-symmetrical interaction, it is advantageous to consider squeezing of light in the momentum quadrature P_L. In other words, $V_{SX} > 1$(it is a consequence of Heisenberg´s uncertainty relation). Larger values of $V_{SX} > 1$ now correspond to more squeezing in momentum, therefore we identify $V_S \equiv V_{SP}$. The function of the logarithmic negativity becomes zero in the infinity of V_N and increases

very slowly with increasing V_S, therefore we have to take into account higher orders of a Taylor series. We used the limit $V_S \to 1^+$. The character is descrribed by

$$\frac{\partial LN}{\partial V_S}|_{V_S=1} = \frac{2K^2}{V_N ln2}. \tag{3.1}$$

An interesting fact appears also when we study the behaviour of LN from the left side, in the closeness of $V_S = 0$. When we apply the first derivative of the logarithmic negativity and then take the limit for $V_S \to 0$ we obtain

$$\frac{\partial LN}{\partial V_S}|_{V_S=0} = \frac{2K^2 V_N}{(V_N^2 - 1)ln2}. \tag{3.2}$$

It means that in the area of higher thermal noise, the LN is increasing faster in the closeness of $V_S = 0$. Considering high values of V_N, (3.2) reduces to (3.1), which would mean that the derivative does not change with V_S, but this would not correspond to Fig. 3.1. Therefore we add here a better approximation of (3.1). We took into account higher orders of Taylor series and obtain $\frac{\partial LN}{\partial V_S}|_{V_S=1} = \frac{2K^2}{V_N ln2} - \frac{8K^4}{V_N^2 ln2}$. If we study the absolute value of entanglement in the area of high V_N with no squeezing for a weak interaction, we obtain

$$f_{LN} = -log_2(1 - \frac{2K^2}{V_N}). \tag{3.3}$$

It clearly demonstrates how logarithmic negativity is non-vanishing for large V_N and the possibility to compensate the larger variance by higher interaction strength K.

3.2 ROBUSTNESS OF ENTANGLEMENT FROM QND INTERACTION

An important characteristic of any quantum system is its robustness against energy damping. Since we consider two physically different systems, light and mechanical oscillator, it opens a question in what system the energy damping affects the generation of entanglement more. To involve energy loss in each system we consider simple beam splitter. For this purpose, we derive a condition for the minimum $\eta_{min} \in (0, 1)$, that represents the transmission of the beam splitter. We also include a condition that makes $\eta_{min} \leq 0$ and

therefore the entanglement is robust for all values of $\eta > 0$, we say that the robustness is *absolute*.

Under the consideration of energy damping in mechanical system we derive

$$\eta > 1 - \frac{4V_N}{V_N^2 - 1}, \tag{3.4}$$

which is independent on K and V_S, therefore if we somehow manage the value of $V_N < 2 + \sqrt{5}$ we automatically get entanglement. This expression corresponds to Fig. 3.2. Note, that we do not need to input squeezed V_S. The

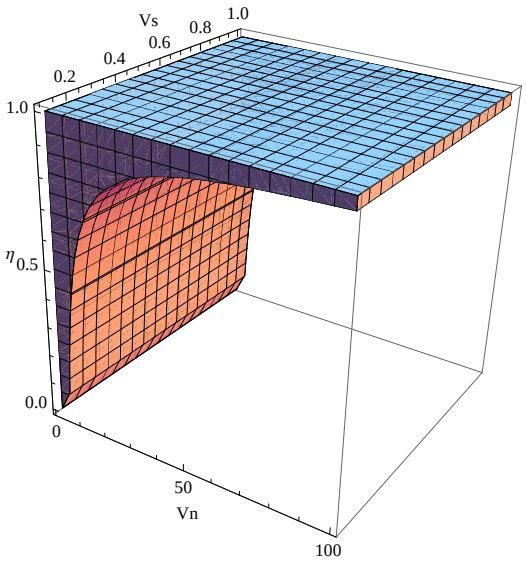

Figure 3.2: QND type of interaction ($K^2 = 0.05$): maximal possible loss of energy in mechanical oscillator to preserve entanglement as a function of V_S and V_N.

area of our main interest is the area of high values of V_N where the condition reduces to

$$\eta > 1 - \frac{4}{V_N}. \tag{3.5}$$

For energy damping in light system, if there is satisfied

$$V_S < \frac{1}{1 + \frac{2K^2 V_N}{\sqrt{K^2 V_N (V_N^2 - 1)}}} \tag{3.6}$$

then the following condition stands, but in other case the entanglement is always robust. The condition for minimum η is

$$\eta > 1 - \frac{4K^2V_S^2V_N}{(V_N^2-1)(V_S-1)^2}, \tag{3.7}$$

which is illustrated in Fig. 3.3. In comparison to (3.4) V_S and K play a substantial role here now. For high values of V_N we obtain from (3.7)

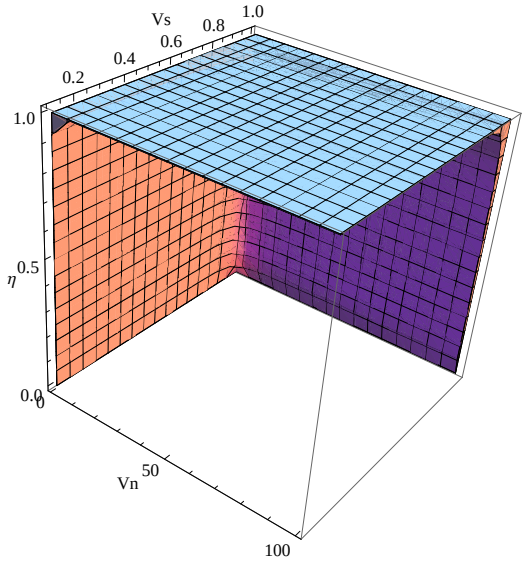

Figure 3.3: QND type of interaction ($K^2 = 0.05$): maximal possible loss of energy in light to preserve entanglement as a function of V_S and V_N.

$$\eta > 1 - \frac{\frac{4K^2V_S^2}{(V_S-1)^2}}{V_N}, \tag{3.8}$$

which is obviously difficult to achieve. The only way to generate it is to increase V_S towards unity for given η. But the appropriate interval of synchronized values of V_S and η is very thin. So squeezed V_S here is disadvantageous.

3.3 CONDITIONAL SQUEEZING FROM QND INTERACTION

In our motivational case of Schrödinger cat experiment the mechanical system can be also conditionally prepared in a non-classical state by a measurement on the quantum system. It can be considered as a transposition of

quantum features to the macro-system which was initially in a very classical state. We focus on studying the conditional variance, especially the case when we are able to squeeze the conditional variance under unity which is called conditional squeezing.

For QND interaction, solving the problem of the conditional variance of the position of the mechanical oscillator leads us to a result that there is squeezing in V_N needed but this is out of possible values of V_N, so there is no chance to obtain $V_{CX} < 1$. On the other hand, $V_{CP} < 1$ is achievable by satisfying

$$V_S < \frac{K^2 V_N}{V_N - 1}. \tag{3.9}$$

In the area of high values of V_N it reduces to

$$V_S < K^2. \tag{3.10}$$

Coexistence of entanglement and $V_{CX} < 1$ is not possible, but entanglement and $V_{CP} < 1$ may be coexisting and that happens if we satisfy the restriction for $V_{CP} < 1$ because generating entanglement for QND is not limitted in our considerated values.

Besides the existence of conditional squeezing of mechanical oscillator we study how much under unity the conditional squeezing goes. As we did in entanglement analysis we identify $V_S \equiv V_{SP}$ here, too. The amount of conditional squeezing can be described by the equation

$$V_{CP} = \frac{V_N V_S}{V_S + K^2 V_N}. \tag{3.11}$$

For better insight we include the illustration in Fig. 3.4. In the area of high values of V_N the Eq.(3.11) changes to

$$V_{CP} = \frac{V_S}{K^2}. \tag{3.12}$$

From Fig. 3.4 and also from (3.12) we can certainly say that V_S plays positive role for obtaining more conditional variance.

All results clearly demontrate that QND type of thermal entanglement between light mode at ground state and mechanical mode at thermal equalibrium not only exists for arbitrary temperature, but also remains reasonably robust and can be exploited in the remote state prepration. It opens a way to possible applications of this thermal entanglement which follows in the next chapter.

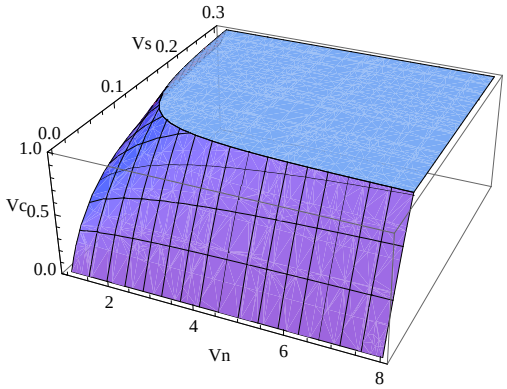

Figure 3.4: QND type of interaction ($K^2 = 0.05$): the dependence of the conditional squeezing V_{CP} on V_S and V_N.

Chapter 4

ANALYSIS OF ENTANGLEMENT MEDIATED BY THERMAL NOISE

In this chapter we are going back to our original motivation presented in the intorduction. Our analysis is focused on deriving conditions that guarantee generating entanglement between systems A and B without directly interacting with each other. Entanglement is mediated by system M in an unknown state. We consider the mediator to be mechanical system and two systems A and B can be two modes of radiation, for example, at different frequencies. Therefore, it can describe the example of quantum transducer between two different frequencies of radiation [19],[20],[21]. The mechanical state can be naturally a thermal state at thermal equlibrium with room temperature. The goal is to find the proper type of interaction to generate entanglement between systems A-M and B-M, respectively. Even more subseqent interactions may be needed. If such a configuration exists, we include quantitative analysis as well. A large attention is paid to a stability of entanglement generation in the presence of small energy absorption during the entangling process. It is very important for final judgement about feasibility of proposed method. Robustness of generated entangled states against subsequent damping before they are used for an application is also discussed. Simple analytical results are rare in this kind of complex non-linear problem. Most results are presented in figures followed by a discussion. Although the problem can be solved analytically, the analytical forms of formulas are too complex to be presented.

4.1 MEDIATED QND INTERACTION

We consider three quantum harmonic oscillators coupled in pairs, see Fig. 4.1(a). Oscillators A, B representing for example optical modes are accessible, they can be prepared in any state and measured by any measurement. Accessible oscillators A, B however do not interact with each other. The coupling is performed by the mediating oscillator M, representing on the other hand a mechanical mode. Each of the oscillators is described by its operators $X = a + a^+$ and $P = i(a^+ - a)$ representing generalized position and momentum. We denote one oscillator X_M, P_M and the two other oscillators X_i, P_i, $i = A, B$. Both the variables satisfy the commutation relations $[X_i, P_i] = 2i$ and $[X_M, P_M] = 2i$ of generalized position and momentum. The mediator M appears in a thermal state with the variance $V_N > 1$ of both X_M, P_M variables. We also consider that V_N is not known and can even fluctuate. Systems A and B can be either at thermal equilibrium state with the variance $V_i > 1, i \in A, B$, or they can be cooled down to a pure state at quantum limit with the variance $V_i = 1$.

The scheme for our analysis consists of three physical systems - two oscillators A and B and one mediating oscillator M. We now let the M system interact subsequently with A and B systems by four unitary QND interactions, as it is shown in Fig. 4.1(b). The interaction is considered to be faster than any relevant decoherence time. It limits naturally the interaction transfer K. The mediator participates in all four interactions - in QND1 and QND3 along with A system and in QND2 and QND4 along with B system. We ignore, for a while, all the elements LOSS1-LOSS7 that will be considered later.

The only arrangement that enables generating entanglement even for high values of V_N (representing ambient temperature) is represented in Heisenberg picture by transformations

$$\begin{aligned} \text{QND1} : X'_A &= X_A - K \cdot X_M \;\; P'_A = P_A, \\ X'_M &= X_M \;\; P'_M = P_M + K \cdot P_A, \end{aligned}$$

$$\begin{aligned} \text{QND2} : X'_B &= X_B \;\; P'_B = P_B - K \cdot P'_M, \\ X''_M &= X'_M + K \cdot X_B \;\; P''_M = P'_M, \end{aligned}$$

$$\begin{aligned} \text{QND3} : X''_A &= X'_A + K \cdot X''_M \;\; P''_A = P'_A, \\ X'''_M &= X''_M \;\; P'''_M = P''_M - K \cdot P'_A, \end{aligned}$$

$$\begin{aligned} \text{QND4} : X''_B = X'_B \;\; P''_B = P'_B + K \cdot P'''_M, \\ X''''_M = X'''_M - K \cdot X'_B \;\; P''''_M = P'''_M, \end{aligned} \tag{4.1}$$

where $X_M(X_i), P_M(P_i), i = A, B$ represent operators of mediator (oscillators A and B), and K stands for the interaction gain. Applying these transformations sequentially leads us to the operation

$$\begin{aligned} X''_A = X_A + K^2 \cdot X_B \quad P''_A = P_A, \\ X''_B = X_B \quad P''_B = P_B - K^2 \cdot P_A, \end{aligned} \tag{4.2}$$

which does not depend on the mediator at all. It is an interesting result because it has the form of QND type of interaction between A and B with the transfer coefficient $\tilde{K} = K^2$. The whole procedure therefore behaves as a single QND interaction between oscillators A and B, even though there is no actual coupling between them. Advantageously, it does not depend on the mediator M, therefore it works even for arbitrary noisy and unstable states of M. The fact that thermal noise of the mediator does not affect the joint operation between the oscillators A and B was the main initial reason to focus on this configuration of four consequent QND types of interaction.

4.2 THE GEOMETRIC PHASE POINT OF VIEW

If a physical system drives around a closed path in phase space, the geometric phase (Berry phase)[22] is imparted on the wavefunction of the quantum state. Wide applications of this phase can be found in quantum computing to create logic gates, but in [11] the connection between geometric phase and optomechanics is presented.

The autors of [11] proposed a method of four subsequent interactions between mechanical and optical resonator, that allows to generate squeezed state of the mechanical one. This configuration also leaves the resulting state of the oscillators disentangled. If we realize the analogy between the problem in this master´s thesis and the method in [11], the motivation becomes clear. By adding a third system, the configuration generates two mode squeezing - entanglement between two systems, whereas the third one - mediator is disentangled. In [11], the authors disentangled light mode, here we however focus on more interesting and logical case of disentanglement of noisy mechanical mode. The non-existing correlations between the systems bring

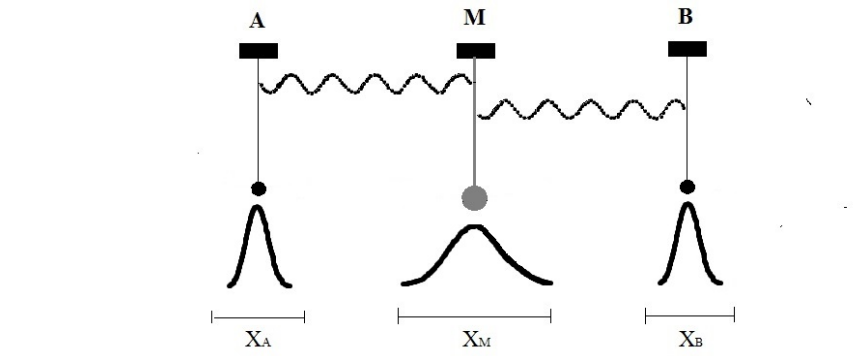

(a)

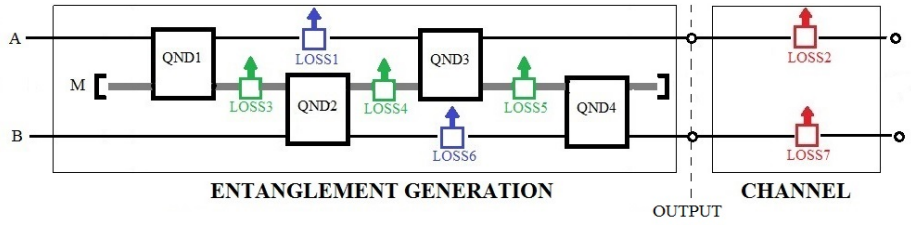

(b)

Figure 4.1: (a) The basic idea of three coupled harmonic oscillators. (b) The scheme of entangling procedure. Accessible oscillators A, B are sequentially coupled to not accessible system M by interactions QND1-QND4. Each oscillator experiences energy damping through the process and in the consequent channel represented by the elements LOSS1-LOSS7. Three colours of these elements are used to illustrate different types of energy loss depending on where it is considered. Blue colour corresponds to η_{AB}, green colour corresponds to η_M, whereas red colour illustrates the influence of energy damping in the ouside channel η_{CH}. We study the generation of entanglement at the output and its robustness to energy loss at the outside channel.

the possibility of generating entanglement independently on the mediating system. Then the mediator can be in any state, even classical thermal state at a room temperature and entangling procedure will work. In addition, the mediator does not have to be measured after the entangling procedure. The goal is to find proper interactions that correspond to this idea of implementing the geometric phase on the mediator.

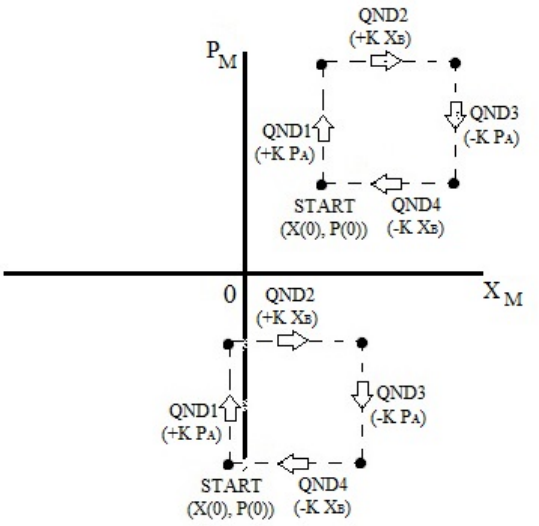

Figure 4.2: The evolution of the mechanical system in phase space. Dashed lines represent the optomechanical interactions between mechanical oscillator and optical mode A or B. Two random starting points are shown. The whole procedure consisting of four QND interactions (A-M, B-M) produces a closed loop in phase space, no matter where the starting point is. The whole procedure behaves as an interaction between two optical modes A and B, whereas the mechanical oscillator is left out.

4.3 MEDIATED GENERATION OF ENTANGLEMENT

After the entangling procedure at Fig. 4.1(b), the QND interaction advantageously produces entanglement for all the possible values of K for $V_{A,B} = 1$ [18]. The smallest symplectic eigenvalue of the covariance matrix in idealized case with no loss of energy and $V_{A,B} = 1$ is given by

$$\nu_-^0 = \sqrt{1 + 2K^4 - 2\sqrt{K^4 + K^8}}. \tag{4.3}$$

In the ideal case of unitary interactions, the transfer coefficient K is only factor that determines the amount of entanglement. The entanglement does not depend on the state of mediator M. As it is easy to see from Fig. 4.3, if we assume $V_i = 1$, $i \in A, B$, increasing transfer coefficient K simply guarantees more entanglement.

However, if oscillators A, B are not cooled down to the ground state and they contain initially thermal state with $V_A = V_B = V_T > 1$, the resulting

smallest symplectic eigenvalue takes the form

$$\nu_-^T = V_T \cdot \nu_-^0. \tag{4.4}$$

Unlike in the case with $V_{A,B} = 1$, here we are limited by condition for the interaction gain

$$K > \sqrt{\frac{V_T^2 - 1}{2V_T}}. \tag{4.5}$$

Using the expansion to the second order for $V_T \gg 1$ we obtain the condition for observing entanglement $V_T < 2K^2$. It means that it is still possible to obtain entangled states just by increasing the interaction gain above threshold $K_{TH} = \sqrt{\frac{V_T}{2}}$, even if there are only noisy systems far from being in the ground state.

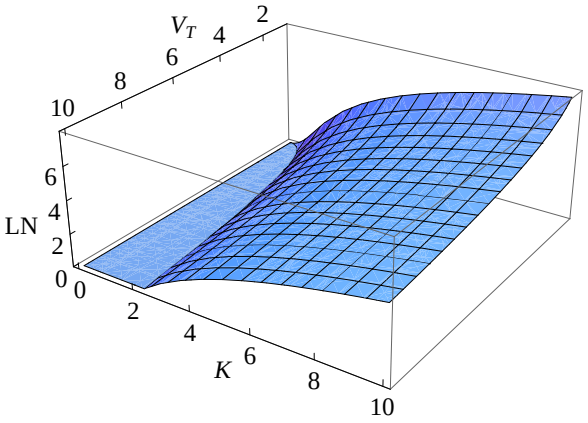

Figure 4.3: The amount of produced entanglement dependent on the interaction gain K and on the noise of side oscillators V_T if the whole process does not experience any loss of energy.

The dependence of logarithmic negativity LN on V_T and K is shown in Fig. 4.3. As long as we satisfy (4.5), increasing value of K guarantees more entanglement which is the same result as we faced above for $V_{A,B} = 1$. It was verified by semi-positiveness of $\frac{\partial LN}{\partial K}$ for any $V_T > 0$ and increasing $K > 0$. Simultaneously, LN descreases for any $K > 0$ and increasing V_T, it proves that higher thermal noise in systems A, B lowers the amount of produced entanglement for any given value of K.

4.4 ROBUSTNESS OF GENERATED ENTANGLEMENT

An important characteristic of any entangled states is a robustness against an energy damping. We discuss the case when the whole entangling procedure is assumed to be perfect and we consider only loss of energy at the output to determine robustness of the entanglement. In Fig. 4.1(b), it means removing all the damping placed inside the generation scheme except of LOSS2 and LOSS7 presented in the channel. The energy damping can be simulated by implementing an auxiliary beam splitting type of interaction with ancillary environmental oscillators in ground states. This interaction is characterized by its transmission $\eta \in (0;1)$. The operators of oscillators A, B therefore change to a new form

$$\begin{aligned} X_i' &= \sqrt{\eta_i} X_i + \sqrt{1-\eta_i} X_{0i}, \\ P_i' &= \sqrt{\eta_i} P_i + \sqrt{1-\eta_i} P_{0i}, \end{aligned} \tag{4.6}$$

where $i \in A, B$. To simplify analysis we take the same $\eta_2 = \eta_7 = \eta_{CH}$ for both of the systems A, B. If we assume both oscillators A, B in a quantum limit with $V_{A,B} = 1$, the condition that has to be satisfied takes the form

$$\eta_{CH} > 1 - \frac{2}{K^2}. \tag{4.7}$$

This is a very positive outcome in the meaning that for $K < \sqrt{2}$ the generated entanglement is absolutely robust. On the other hand, the amount of robust entanglement is not very large, because of this limit (4.7) to guarantee robustness; see Fig. 4.4. Since for the ideal unitary entangling procedure the generated state does not depend on M, there is also no dependence on the mediator in (4.7).

The threshold depicted in Fig. 4.4 is clearly corresponding with (4.7). On the other hand, considering finite energy losses at the output of entangling procedure makes LN dependent on interaction transfer K. Increasing K no longer guarantees monotonously increasing generation of more entanglement for given value of η_{CH}. The optimal value of interaction transfer K that guarantees the largest amount of entanglement is

$$K = \frac{1}{\sqrt[4]{1-\eta_{CH}}}. \tag{4.8}$$

As η_{CH} decreases, the optimal K reduces to unity. The sensitivity of Gaussian entanglement to the energy damping depends on how far the oscillators

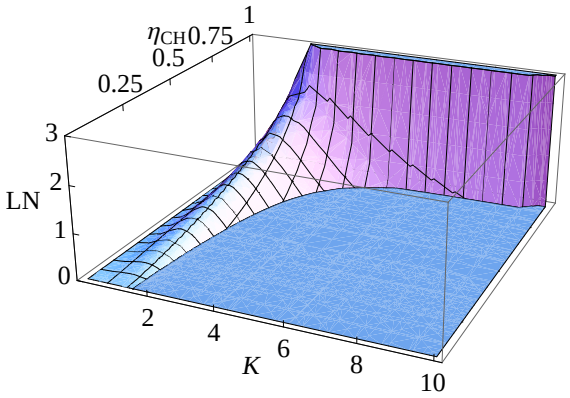

Figure 4.4: The logarithmic negativity of produced entanglement dependent on the loss of energy at the output described by transmission $\eta_2 = \eta_7 = \eta_{CH}$ and on the interaction gain K for $V_i = 1$. We ignore the possibility of energy damping in the process.

are from the ground state. If oscillators A, B are in a thermal state with variance $V_T > 1$, the maximal possible energy damping at the output to preserve entanglement is presented in Fig. 4.5. In the area $\eta_{CH} = 1$, the threshold

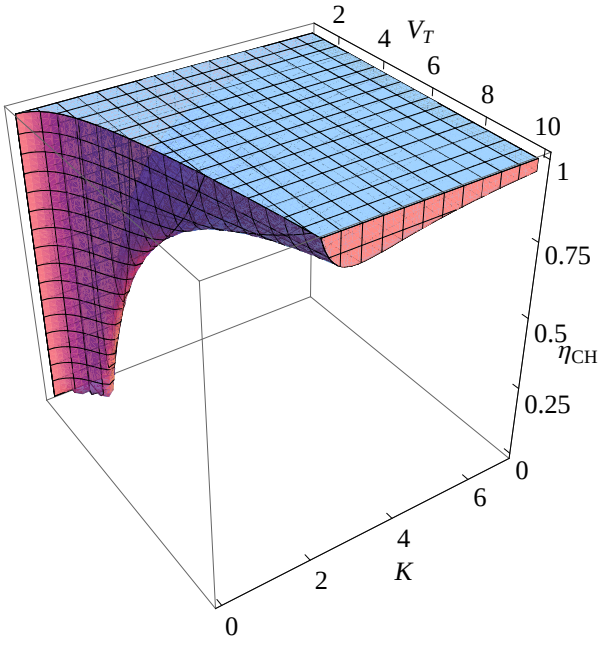

Figure 4.5: Maximal possible loss of energy at the output η_{CH} to preserve entanglement as a function of the interaction gain K and the variance V_T. We assume that the process is without losses.

in Fig. 4.5 is in agreement with the condition (4.5). In general, to preserve entanglement for larger variance V_T in oscillators A, B, only small energy damping ($\eta_{CH} \approx 1$) can be tolerated. That tolerance moreover decreases for larger transfer coefficient K. For every given value of V_T there is however an optimal K that is the least sensitive to the energy damping at the output of the entangler. The optimal value of the interaction gain K is different for every value of V_T. The exact value of optimal K can be found numerically. For not too large $V_T > 1$, there is still a sufficient tolerance of the generated entanglement to damping η_{CH}, if K is optimized.

4.5 LOSS OF ENERGY IN THE ENTANGLING PROCESS

In principle, no physical system is perfect in the sense of preserving energy through any processes. It is therefore crucial to test robustness of the entangling procedure to small energy dissipation especially in the limit of large V_N of the mediator M. To emulate impact of small dissipation from both A, B oscillators and mediator M as well, we use a (4.6) with $i = 1, 3 - 6$. We consider such the dissipation of energy after every QND interaction in each system; see Fig. 4.1. It physically models non-unit in-coupling and out-coupling efficiencies that are also realistically limiting interactions between different systems. It is now useful to distinguish in our following discussions the small energy dissipation in the process of generating entanglement from the analysis of robustness of generated entanglement against the energy damping. We therefore consider either $\eta_1, \eta_3, \eta_4, \eta_5, \eta_6$ inside the entangling process or $\eta_2, \eta_7 = \eta_{CH}$ after the entangling process, respectively. We consider for this section $\eta_{CH} = 1$. The energy dissipation in the process is described by unified parameter $\eta = \eta_1 = \eta_3 = \eta_4 = \eta_5 = \eta_6$ for simplicity. We do not consider any damping before the entangling process for all the systems A, B and M. The initial states are classical (ground state, thermal state) and therefore, such damping can be involved into the variances of that states.

Let´s begin with the situation when the systems A, B are cooled down to the ground states with $V_i = 1$, $i = A, B$. If we use the expansion for $\eta \approx 1$ and $K \gg 1$ the dominant element of the minimal symplectic eigenvalue ν_- is $\frac{3K^2}{4}(1 - \eta)$. For $\eta < 1$, when K increases, the minimal symplectic eigenvalue grows and reaches $\nu_- > 1$, for some K. It means that considering a small losses in the process qualitatively influences the generation of entanglement. Increase of K therefore no longer guarantees more entanglement, but at some

value of K the logarithmic negativity starts decreasing and reaches the point of no entanglement at all, as is depicted in Fig. 4.6. The optimal K has to be found numerically. It is an example why the test of robustness against basic energy damping is important to verify stability of the entangling process.

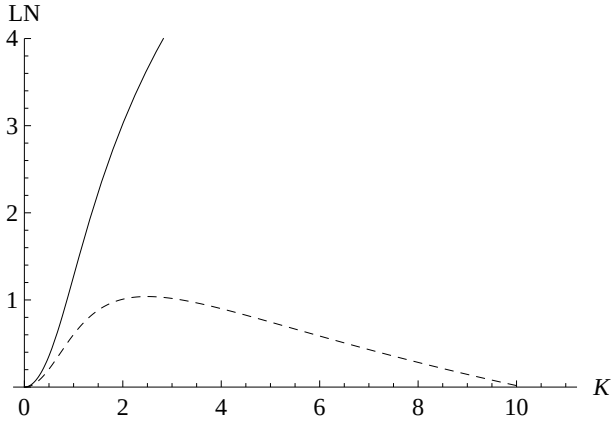

Figure 4.6: The dependence of logarithmic negativity on the interaction gain K. Full line stands for the case with no losses considered. Dashed line characterizes the bahaviour with $\eta = 0.95$, $V_N = 10^3$, $V_i = 1$ considered.

In Fig. 4.7(a) and Fig. 4.7(b) we present the previous effect for small and large V_N for easier insight as the function of K. For the ground state $V_N = 1$ of the mediator, even very small K is not able to compensate arbitrary losses in the process. To generate entanglement there is still a clear threshold to be overcome, which we can see in Fig. 4.7(a). Both Figs. 4.7(a) and 4.7(b) show that increasing interaction gain K makes the condition for generation of entanglement more strict so the energy dissipation in the process has to be small. Large variance V_N restricts the appropriate range of η that guarantees generation of entanglement, as it is visible at Fig. 4.7(b). However, still for large $V_N \gg 1$ we are able to produce entanglement if the dissipation $\eta \approx 1$ is moderate and transfer coefficient K is small. Evidently, this sensitivity of the entangling process for large V_N is example of crucial importance of the analysis of robustness of the entangler against the small energy dissipation.

When the systems A, B are out of ground states, it appeared also to be crucial in the analysis of robustness. We consider now the oscillators A, B being in a thermal state with the variance V_T and continue the discussion of energy damping in the process. The case when systems A, B are in thermal states can be understood from Fig. 4.8. We used the large value of variance $V_N = 10^3$ for the mediator, but all qualitative results mentioned here can be generalized for all values of V_N. We also used a different scale for η to visualize

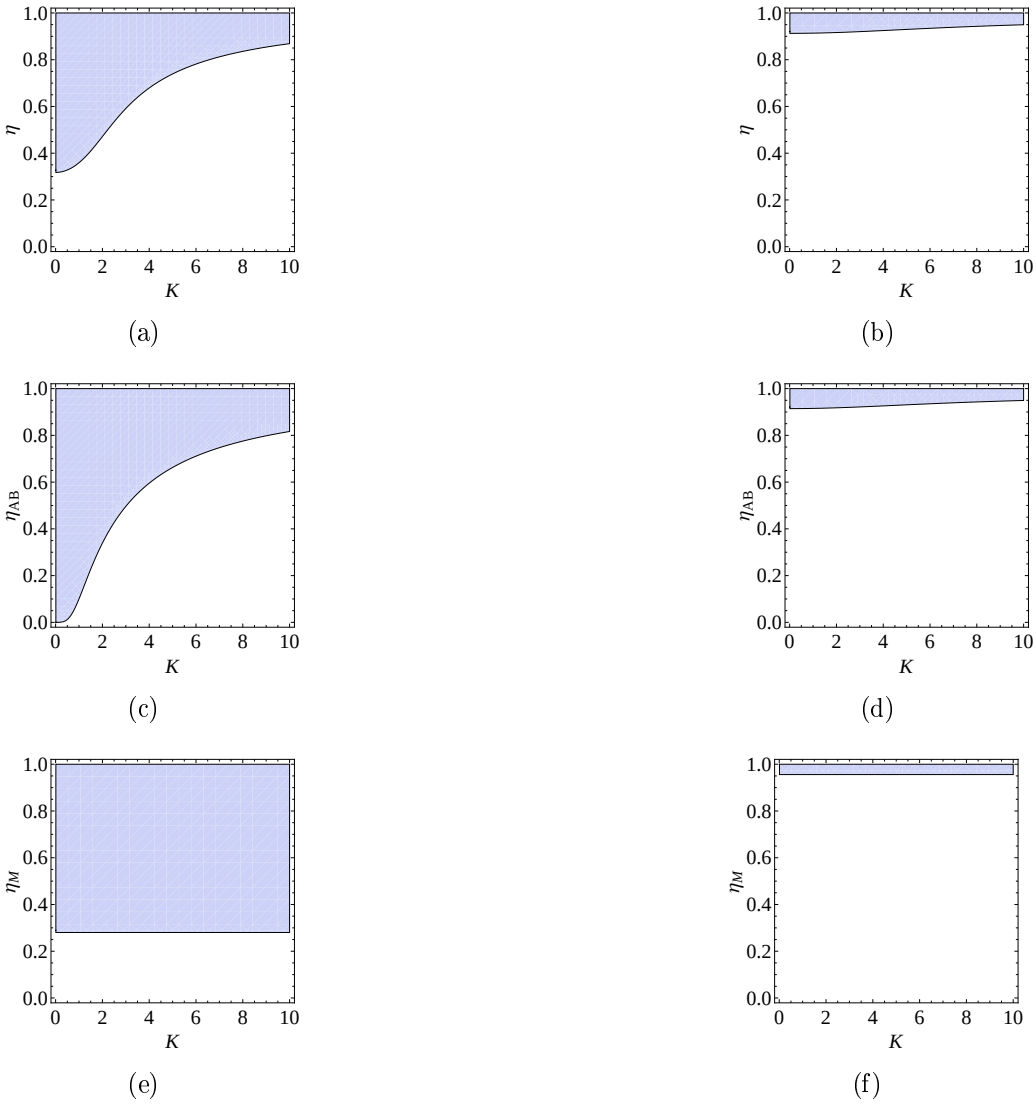

Figure 4.7: Maximal possible loss of energy in the process to generate entanglement at the output as a function of the interaction gain K. Areas of $V_N = 1$ (left column) and $V_N = 10^3$ (right column) are shown for three different types of considered losses. Figures (a) and (b) illustrate equal losses in the process $\eta_{1,3,4,5,6} = \eta$, (c) and (d) show the result if the damping $\eta_{AB} = \eta_{1,6}$ is held by only A, B systems, whereas (e) and (f) stand for damping $\eta_M = \eta_{3,4,5}$ held by only mediator M. We kept $V_i = 1$.

the desired effect. The upper area for $\eta \approx 1$ again corresponds to (4.5). The left side of Fig. 4.8 ($V_T \approx 1$) can be easily matched with Fig. 4.7(b). Clearly, for larger $V_T > 1$, the tolerance to smaller η vanishes. It happens even more rapidly, when K is very large. We would like to stress that every value of V_T has however an optimal, yet different, value of K that determines the maximal energy dissipation in the process. We faced a similar feature of the different optimal value of K for each V_T in the robustness analysis against channel damping, see Fig. 4.5. It is therefore useful to cool the accessible systems A, B down before the entangling process, it improves the robustness against the dissipation during the less controllable entangling process.

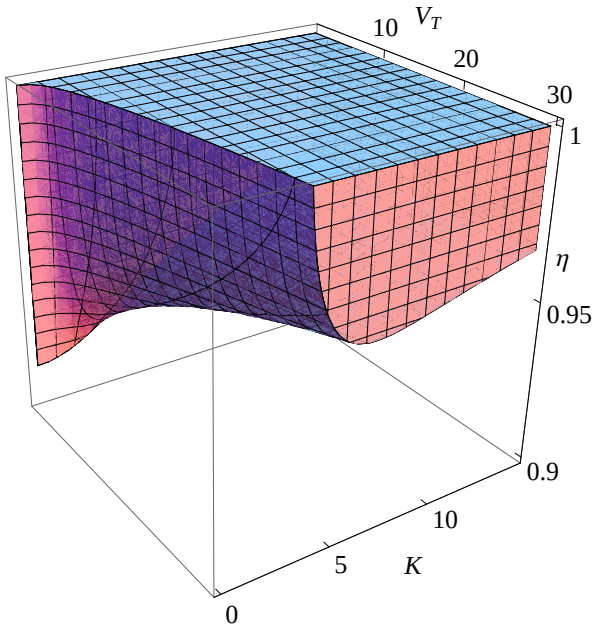

Figure 4.8: Maximal possible loss of energy in the process η to generate entanglement as a function of the interaction gain K and the variance V_T. We used $V_N = 10^3$.

4.6 LOSS OF ENERGY VIA OSCILLATORS A, B

We divide our discussion of generating entanglement in separate categories to understand the influence of small loss of energy during the process depending on where it is considered. Let us first assume that the mediator does not

experience any loss of energy, therefore the imperfectness is held by systems A and B, with the same η_{AB} for both for simplicity $\eta_{AB} = \eta_1 = \eta_6$.

We begin with the systems A, B at the ground state $V_i = 1$, $i \in A, B$. In Figs. 4.7(c) and 4.7(d) one can see the negative role of increasing K and V_N. The function has a similar character as in Figs. 4.7(a) and 4.7(b) but here we are able to produce entanglement even for larger losses by decreasing K for low thermal noise. In fact, Fig. 4.7(c) shows that for ground state $V_N = 1$, when K is small enough, entanglement is generated for all values of $\eta_{AB} > 0$. This is a feature which can be observed for classical ground states of A, B and M. Using Taylor series we again verified the possibility of generating entangled states even for $V_N \gg 1$ by keeping K and η_{AB} very low.

To present how much entanglement is generated we include Fig. 4.9(a), where logarithmic negativity is shown. We can see that for given η_{AB} the largest logarithmic negativity LN appears for an optimal value of K. This optimal value of K once more decreases for smaller η_{AB}. We stated above for equal losses in all the systems during process that even small dissipation of energy breaks the monotonous increase of logarithmic negativity which applies also here for the dissipation considered only in oscillators A, B. Theoretically perfect process produces more entanglement for higher K, but considering finite losses equally just in systems A, B destroys this possibility and entanglement reaches its maximum and then drops down with increasing K.

To illustrate the influence of $V_T > 1$, when A and B are not cooled down to the ground states, on the existence of entanglement we present Fig. 4.10(a), which we produced by taking a concrete configuration with $V_N = 10^3$. We used a different scale for η_{AB} to stress the importance of how much precise the process has to be to observe entanglement. Fig. 4.10(a) and Fig. 4.8 appear nearly identical, but numerical verification shows a slight difference. Nevertheless, all the qualitative conclusions apply here as well, although the dissipation is present only in the systems A and B. Increasing thermal noise V_T generally tolerates less dissipation in the systems A and B and interaction gain K has a different optimal value for each V_T. The resemblance between the situation where the energy dissipation in oscillators A, B only and the situation with equal dissipation in all the systems indicates that systems A, B are probably less robust against energy losses during the production of entanglement. This statement holds for both ground state value $V_T = 1$ and $V_T > 1$ far from the ground states of A and B.

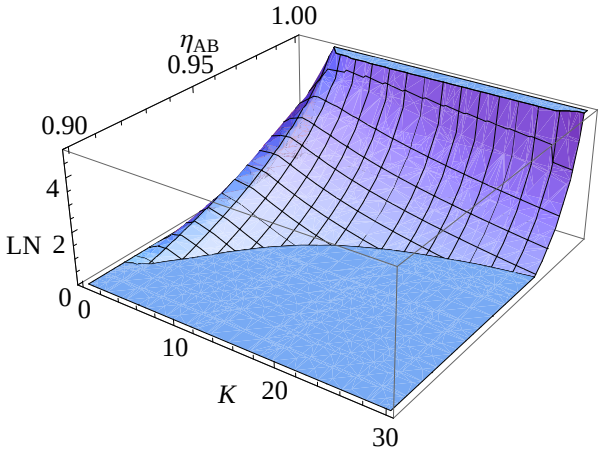

(a)

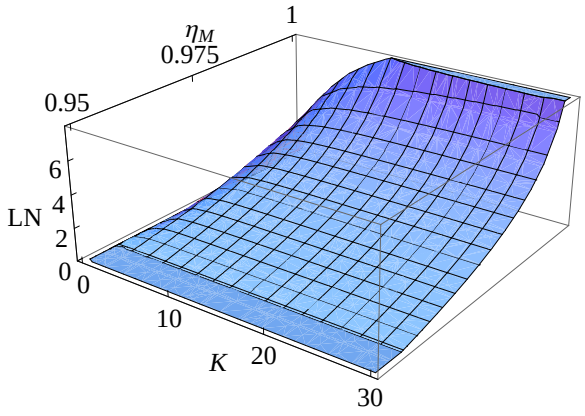

(b)

Figure 4.9: The amount of generated entanglement as a function of the interaction gain K and energy dissipation η_i. The energy loss η_i is considered either only in oscillators A, B (a) or only in the mediator M (b). We used $V_N = 10^3$ and $V_i = 1$.

4.7 LOSS OF ENERGY VIA THE MEDIATOR

We now discuss the second case when the loss of energy is assumed only in the mediator which means taking into account LOSS3, LOSS4 and LOSS5 in Fig. 4.1 with the same $\eta_M = \eta_3 = \eta_4 = \eta_5$. The bahaviour of the function is illustrated in Figs. 4.7(e) and 4.7(f). Typically, entanglement vanishes with increasing V_N. As it was for previous cases, even here keeping η_M close to unity (low damping) enables to observe entanglement even for high thermal noise, which was verified by expansion for $V_N \gg 1$. The difference appears when we study the role of K which has no practical effect on the generation of entanglement in this case. We can see that there is a clear threshold in the value of η_M for each value of V_N. Exact value of the threshold has to be approached numerically.

The amount of entanglement as the function of K is presented in Fig. 4.9(b), where one can see a very different character of the function than in Fig. 4.9(a). Here after reaching the optimal value of K, the amount of entanglement does not drop but saturates with increasing K. Typically, energy dissipation η_M approaching zero makes the entanglement vanish.

Fig. 4.10(b) illustrates the influence of thermal noise $V_T > 1$. Increasing thermal noise in systems A, B has negative influence in the sense that we need stronger interaction gain K. However, once the appropriate value of K to generate entanglement is reached for η_M in the process, further increasing of K does not destroy entanglement. In fact, in Fig. 4.10(b) one can see that the function shows saturation for increasing K and even in the direction of increasing V_T. Finding the exact saturation value has to be approached by numerical analysis. The saturation in the interaction gain K and even in thermal noise V_T is opposite to previous cases, where entanglement was very sensitive to the change of both K and V_T. The major qualitative difference between Fig. 4.10(b) and Fig. 4.8 just proves our earlier conclusion that the energy damping in systems A, B disturbs the entanglement generation more than in the mediator M. The damping process in A and B is therefore dominant, it determines overall features of the robustness against energy damping in the entangling process and practically determines the optimal numerical value of K to generate maximum of entanglement.

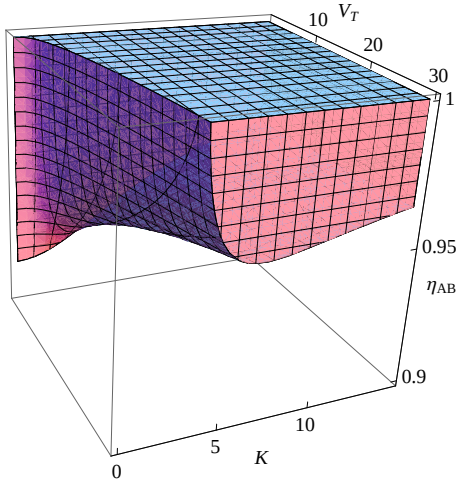

(a)

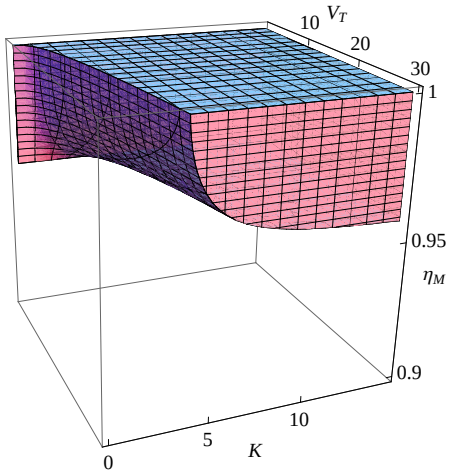

(b)

Figure 4.10: Maximal possible loss of energy to generate entanglement as a function of the thermal noise V_T and the interaction gain K. Figure (a) illustrates the influence of losses being considered only in systems A, B, whereas (b) stands for losses held by only mediator M. We kept $V_N = 10^3$.

4.8 ROBUSTNESS OF ENTANGLEMENT GENERATED IN THE PROCEDURE WITH SMALL DISSIPATION

So far, we used various idealizations to properly analyze different influence of energy damping and their influences on the production of entanglement. Now, we keep the small dissipation of energy in each system between subsequent QND interactions in the procedure and will investigate how much the produced entanglement in the systems A and B is robust against energy loss in the channel. We consider $\eta_{AB} = \eta_M = 0.98$ ($\eta_{1,3,4,5,6} = 0.98$ in Fig. 1(b)). We also unify the losses at the output $\eta_{CH} = \eta_{2,7}$ and analyze the robustness of generated entanglement for different η_{CH}. In Fig. 4.11 we

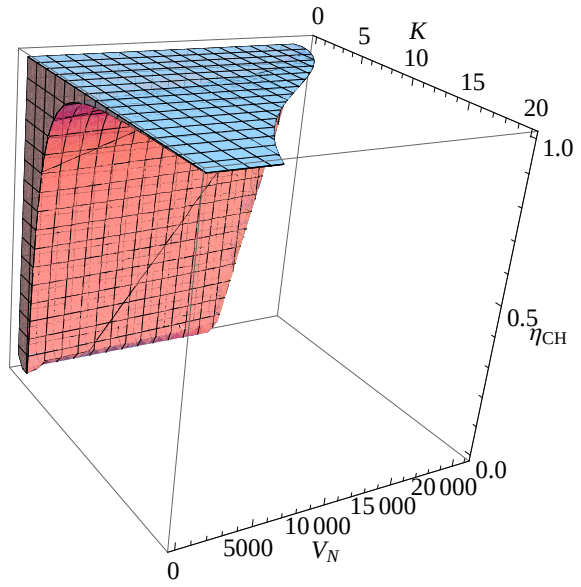

Figure 4.11: Maximal possible loss of energy at the output η_{CH} to preserve entanglement as the function of thermal noise V_N and the interaction gain K. We assume equal loss of energy during the process $\eta_{1,3,4,5,6} = 0.98$ and keep $V_i = 1$.

present that generated entanglement can be preserved for any η_{CH} even for increasing thermal noise V_N, if the interaction transfer K is lowered enough. The relation between V_N and η_{CH} is strongly determined by the value of K, which is separately shown in Fig. 4.12. Unlike in previous situations, here we face a clear maximum of V_N to preserve entanglement after the channel. The minimal η_{CH} to preserve entanglement increases for large K. Black line in

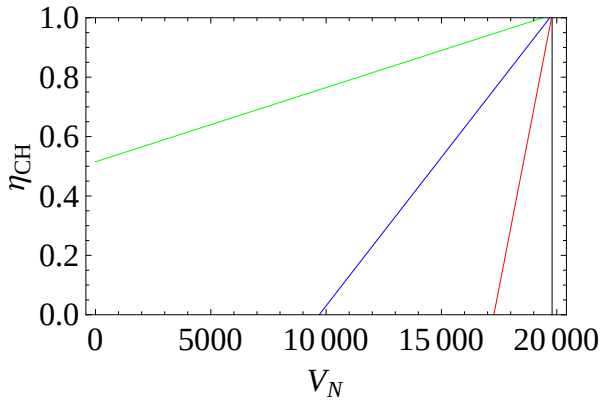

Figure 4.12: Maximal possible loss of energy at the output η_{CH} to preserve entanglement as a function of thermal noise of the mediator V_N if the process expreriences 2% energy loss and systems A, B are in a state with variance $V_i = 1$. It is shown for different values of the interaction gain K: $K = 0.01$(black), $K = 0.5$(red), $K = 1$(blue), $K = 2$(green)

Fig. 4.12 shows that keeping interaction transfer K low enough makes entanglement absolutely robust against output dissipation even for noisy system M. It reaches the same robustness inside the channel as in the ideal case depicted in Fig. 4.4. The absolute robustness vanishes with higher values of K. Keeping the interaction transfer K low enables to compensate the loss of energy by lowering thermal noise in the mediator M, green line illustrates that increased value of K destroys the absolute robustness.

The logarithmic negativity of generated entanglement passing the channels is presented in Fig. 4.13. This graph was obtained by using $V_N = 10^3$ and $V_i = 1$, $i \in A, B$. It shows that even combining small dissipation in the process and energy loss at the output does not destroy the main idea of the entangler mediated by very noisy oscillator. To produce the largest logarithmic negativity LN we have to achieve an optimal value of K which is different for each η_{CH}. The amount of entanglement decreases along with the efficiency at the output η_{CH}, however, comparing to Fig. 4.4 shows that the absolute robustness does not vanish for small dissipation in the entangling process. For the systems A and B initially in the ground states, the entangling procedure is stable against small energy dissipation during process and generates absolutely robust entanglement, when transfer coefficient K of the QND interactions is optimized.

To complete our analysis we present the dependence of entanglement on increasing thermal noise V_T in oscillators A, B. The function in Fig. 4.14

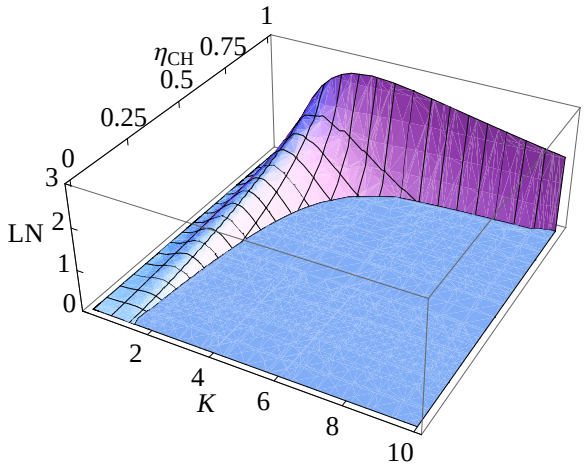

Figure 4.13: The logarithmic negativity of preserved entanglement as a function of interaction gain K and the loss of energy at the output η_{CH}. We assume equal loss of energy during the process $\eta_{1,3,4,5,6} = 0.98$ and fix $V_i = 1$ and $V_N = 10^3$.

shows a similar progress as functions in Fig. 4.5, Fig. 4.8 or Fig. 4.10. All these figures represent different types of dissipation, but the results show a similar relation between interaction gain K and thermal noise V_T. We can see a characteristic feature of the optimal value of K which needs to be optimized for each V_T. Increasing noise in A, B systems forces us to keep η_{CH} in the channel close to unity in order to be able to preserve entanglement.

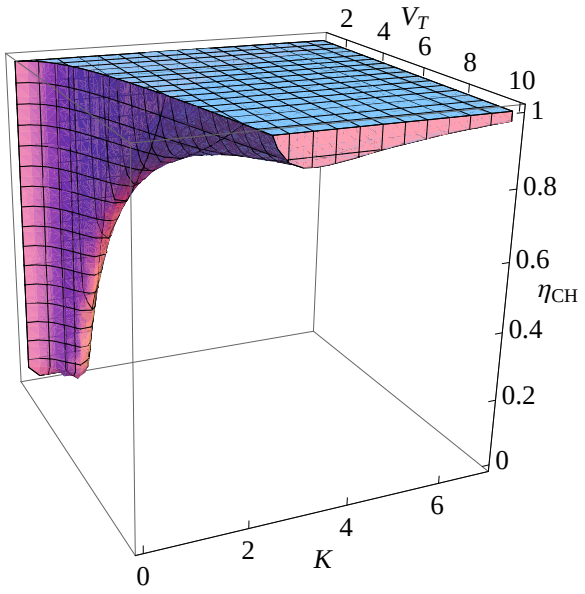

Figure 4.14: Maximal possible loss of energy at the output η_{CH} to preserve entanglement as the function of thermal noise V_T and the interaction gain K. We assume equal loss of energy during the process $\eta_{1,3,4,5,6} = 0.98$ and keep $V_N = 10^3$.

Chapter 5

CONCLUSION AND EXPERIMENTAL PROPOSAL

We suggested the continuous-variable entangling procedure generating arbitrary large amount of entanglement between two oscillators through the mediating oscillator initially in any state. We can now go back to general picture depicted in Fig. 4.1(b). The strength of interaction is powering the amount of Gaussian entanglement. The idealized procedure with zero energy damping generates entanglement that is completely independent on the mediating system and can be absolutely robust against channel dissipation. We determined the threshold value of the interaction strength, that guarantees absolute robustness of generated entanglement against energy damping in the output channels. However, it is crucial to test stability and robustness of the procedure against even small energy damping during the entangling process.

Considering energy damping during the process makes the generation of entanglement strongly determined by the noise initially in the mediating oscillator. Unlike in the idealized case where entanglement increases with stronger interaction of oscillators, considering energy damping during the process shows that entanglement maximum is reached for optimal value of interaction strength. If the entangling process experiences small energy dissipation, the absolute robustness against outside energy damping occurs, but it is limited by the interaction strength and also by the mediating system. We provided the comparison of two different cases depending on where the energy is absorbed during the entangling procedure. The huge impact of energy damping in systems A, B on the generation of entanglement proved their major significance over the damping in the mediator.

The suggested method of generation of Gaussian entanglement between two oscillators mediated by the noisy oscillator is therefore stable against

a small energy damping. After an optimization of the interaction strength, it qualitatively approaches the ideal method without any dissipation. It can stimulate many principal ways how such the entangling procedure can be implemented as quantum transducer between various physical platforms which do not interact directly. A prominent example appears in quantum optomechanics, where the mediator is a mechanical system. The methods allow to reach the basic entangling gate between the systems not interacting directly, but interacting with the mechanical oscillator, without the need to deeply cool it down.

We also include a brief proposal of the experimental configuration that could confirm our theoretical results. The experiment consists of four subsequent QND interactions between light and mechanical oscillator. The basic idea of the experiment corresponds to [11], which is the generation of geometric phase, here imparted on the mechanical oscillator. The modification of [11] consists of adding a third system, which is illustrated in Fig. 5.1. A co-

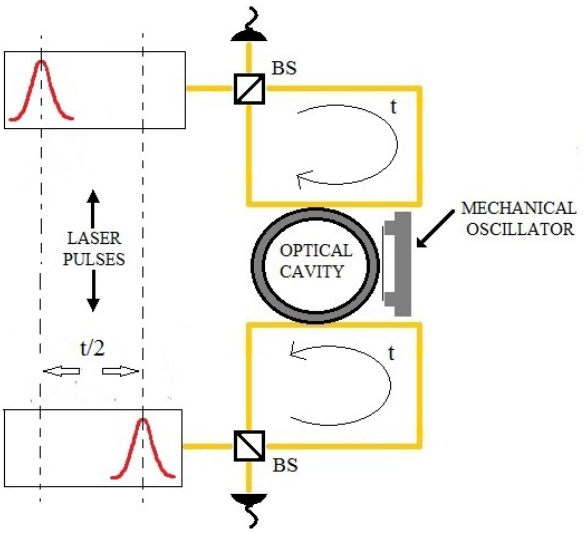

Figure 5.1: The scheme of proposed experiment. Laser pulses interact with the mechanical oscillator via evanescent coupling from a toroidal cavity. The mechanical oscillator acts as a mediator of entanglement between two optical modes by switching the interaction between them.

herent laser pulse of temporal width σ enters the fiber cavity with round trip time t via a beam splitter. The second laser is delayed by factor $t/2$. After one successful laser pulse is coupled to the mechanical resonator via evanescent

wave from a toroidal cavity [23] with decay rate κ, the interaction is switched to the other system and the coupling is performed between mechanical oscillator and the second system. Each interaction switch is accompanied by proper implementation of phase shift in order to perform interactions corresponding to (4.1). Each pulse repeats the cycle and interacts twice with the mechanical oscillator to accomplish four QND subsequent interactions in total, corresponding to Fig. 4.1(b). Therefore the whole scheme behaves like entangling procedure between two optical fields, totally independent on the mechanical oscillator. A modification of the experimental requirements (2.15) apply here, too

$$T_M \gg t > 4\sigma > \kappa^{-1}.$$

This suggested method can be extended to other experimental platforms.

Bibliography

[1] *www.fyzika.jreichl.com/main.article/view/740 − schrodingerova − kocka*

[2] *www.plato.stanford.edu/entries/qt − epr/*

[3] ASPELMEYER, Markus, et al. Cavity optomechanics, arXiv:1303.0733 (2013)

[4] *www.commons.wikimedia.org/wiki/File : CavityOptomechanics.png*

[5] SCULLY, M. O. and ZUBAIRY, M. S. Quantum optics. Cambridge University Press, 1997. 630 p. ISBN 0 521 43595 1

[6] VEDRAL, Vlatko. Modern foundations of quantum optics. Imperial College Press, 2005. 222 p. ISBN 1-86094-553-8

[7] SAKURAI, J. J. Modern Quantum Mechanics(Revised Edition). Addison-Wesley Publishing Company, 1994. 500 p. ISBN 0-201-53929-2

[8] VANNER, M. R., et al. Pulsed quantum optomechanics, arXiv:1011.0879 (2011)

[9] VANNER, M. R., et al. Cooling by measurement and mechanical state tomography via pulsed optomechanics, Nature Communications 4, Article number: 2295 (2013)

[10] BRAWLEY, G. A., et al. Non-linear optomechanical measurement of mechanical motion, arXiv:1404.5746 (2014)

[11] KHOSLA, K. E., et al. Quantum state preparation of a mechanical resonator using an optomechanical geometric phase, New J. Phys. 15 043025 (2013)

[12] McKENZIE, Kirk, et al. Recycled Michelson Interferometer for Gravitational Wave Detection, Phys. Rev. Lett. 88, 231102 (2002)

[13] A. FURUSAWA, J. L. Sörensen, S. L. Braunstein, C. A. Fuchs, H. J. Kimble, and E. S. Polzik, Unconditional quantum teleportation, Science 282, 706 (1998).

[14] N. C. MENICUCCI, S. T. Flammia, and O. Pfister, One-Way Quantum Computing in the Optical Frequency Comb, Phys. Rev. Lett., vol. 101, no. 13, p. 130501, Sep. 2008.

[15] muj.optol.cz/bajer/prezentace/sumy.pps

[16] LAURAT, Julien, et al. Entanglement of two-mode Gaussian states: characterization and experimental production and manipulation, Journal of Optics B 7 (2005) S577

[17] ADESSO, Gerardo and ILLUMINATI, Fabrizio, Equivalence between entanglement and the optimal fidelity of continuous variable teleportation, Phys. Rev. Lett. 95, 150503 (2005)

[18] R. FILIP and V. KUPČÍK, Robust Gaussian entanglement with a macroscopic oscillator at thermal equilibrium, Phys. Rev. A 87, 062323 (2013).

[19] DIDIER, Nicolas, et al. Quantum transducer in circuit optomechanics, arXiv:1201.6293 (2012)

[20] ANDREWS, R. W., et al. Bidirectional and efficient conversion between microwave and optical light, Nature Physics 10, 321–326 (2014)

[21] TIAN, Lin, Optoelectromechanical transducer: reversible conversion between microwave and optical photons, arXiv:1407.3035 (2014)

[22] BERRY, M. V., Quantal phase factors accompanying adiabatic changes, Proc. R. Soc. Lond. A 1984 392, 45-57

[23] ANETSBERGER, G., et al. Near-field cavity optomechanics with nanomechanical oscillators, Nature Physics, 5:909-914 (2009)